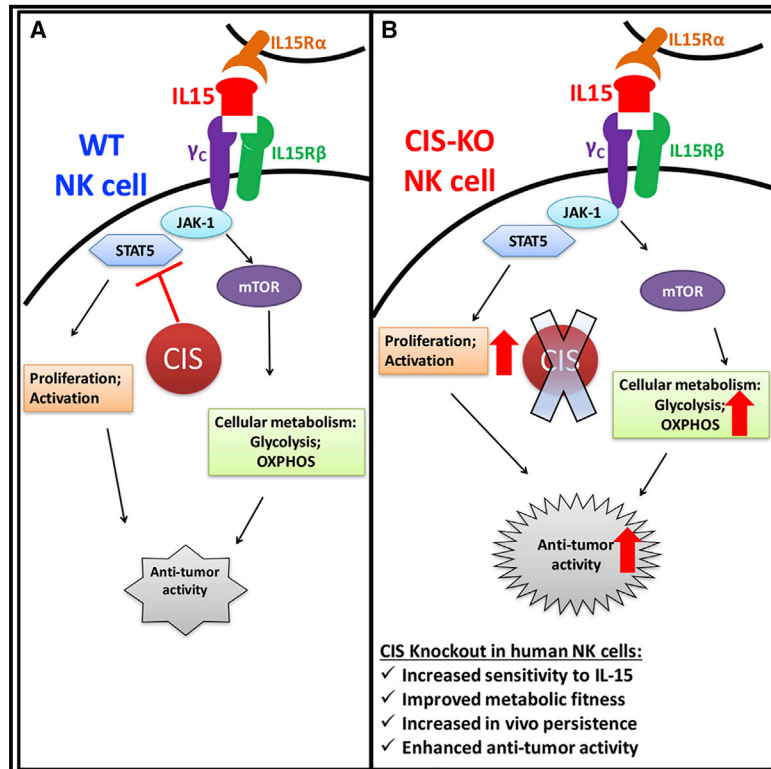


Metabolic Reprogramming via Deletion of *CISH* in Human iPSC-Derived NK Cells Promotes *In Vivo* Persistence and Enhances Anti-tumor Activity

Graphical Abstract



Authors

Huang Zhu, Robert H. Blum, Davide Bernareggi, ..., Kun-Liang Guan, Karl-Johan Malmberg, Dan S. Kaufman

Correspondence

dskaufman@ucsd.edu

In Brief

CISH normally inhibits IL-15 signaling in natural killer (NK) cells. Here, Zhu and colleagues delete *CISH* expression in NK cells derived from human induced pluripotent stem cells (iPSCs). *CISH*^{-/-} iPSC-derived NK cells demonstrate improved killing of tumor cells that is directly attributable to a more efficient metabolic profile.

Highlights

- Deletion of *CISH* in human NK cells leads to improved anti-tumor activity
- *CISH*^{-/-} NK cells demonstrate more efficient glycolytic and OxPhos activity
- The improved metabolic profile is mediated by mTOR signaling
- *CISH*^{-/-} NK cells more effectively treat AML *in vivo* with longer NK cell persistence

Clinical and Translational Report

Metabolic Reprogramming via Deletion of *CISH* in Human iPSC-Derived NK Cells Promotes *In Vivo* Persistence and Enhances Anti-tumor Activity

Huang Zhu,¹ Robert H. Blum,¹ Davide Bernareggi,¹ Eivind Heggernes Ask,³ Zhengming Wu,² Hanna Julie Hoel,³ Zhipeng Meng,² Chengsheng Wu,² Kun-Liang Guan,² Karl-Johan Malmberg,³ and Dan S. Kaufman^{1,4,*}

¹Department of Medicine, Division of Regenerative Medicine, University of California, San Diego, La Jolla, CA, USA

²Department of Pharmacology and Moores Cancer Center, University of California, San Diego, La Jolla, CA, USA

³Department of Cancer Immunology, Institute for Cancer Research, Oslo University Hospital, Oslo, Norway

⁴Lead Contact

*Correspondence: dskaufman@ucsd.edu

<https://doi.org/10.1016/j.stem.2020.05.008>

SUMMARY

Cytokine-inducible SH2-containing protein (CIS; encoded by the gene *CISH*) is a key negative regulator of interleukin-15 (IL-15) signaling in natural killer (NK) cells. Here, we develop human *CISH*-knockout (*CISH*^{-/-}) NK cells using an induced pluripotent stem cell-derived NK cell (iPSC-NK cell) platform. *CISH*^{-/-} iPSC-NK cells demonstrate increased IL-15-mediated JAK-STAT signaling activity. Consequently, *CISH*^{-/-} iPSC-NK cells exhibit improved expansion and increased cytotoxic activity against multiple tumor cell lines when maintained at low cytokine concentrations. *CISH*^{-/-} iPSC-NK cells display significantly increased *in vivo* persistence and inhibition of tumor progression in a leukemia xenograft model. Mechanistically, *CISH*^{-/-} iPSC-NK cells display improved metabolic fitness characterized by increased basal glycolysis, glycolytic capacity, maximal mitochondrial respiration, ATP-linked respiration, and spare respiration capacity mediated by mammalian target of rapamycin (mTOR) signaling that directly contributes to enhanced NK cell function. Together, these studies demonstrate that CIS plays a key role to regulate human NK cell metabolic activity and thereby modulate anti-tumor activity.

INTRODUCTION

Natural killer (NK) cells are an immune effector cell population with an intrinsic ability to kill virus-infected and tumor cells without prior antigen sensitization (Hodgins et al., 2019; Miller and Lanier, 2019; Morvan and Lanier, 2016; Zhu et al., 2018). NK cell-mediated cytotoxicity is regulated by integrating signals from a repertoire of activating and inhibitory receptors (Miller and Lanier, 2019). Activated NK cells can kill target cells through different mechanisms, including release of preformed cytolytic granules and proinflammatory cytokines, as well as triggering cell apoptosis through death-receptor pathways by inducing death ligands such as FAS ligand and TRAIL (Miller and Lanier, 2019; Morvan and Lanier, 2016).

Clinical trials have shown allogeneic primary NK cells from peripheral blood (PB-NK) and umbilical cord blood (UCB-NK) to be safe without causing significant toxicity, such as cytokine release syndrome (CRS), neurotoxicity, or graft-versus-host disease (GVHD) (Dolstra et al., 2017; Geller et al., 2011; Miller and Lanier, 2019; Miller et al., 2005; Romee et al., 2016). Although allogeneic NK cells have been shown to possess potent anti-AML (acute myelogenous leukemia) activity, their efficacy for treating solid tumors has been limited (Hodgins et al., 2019; Miller and Lanier, 2019). One of the major reasons is that adop-

tively transferred primary NK cells typically persist *in vivo* for a relatively short period of time, limiting their anti-tumor efficacy. Unlike autologous chimeric antigen receptor (CAR)-T cell-based therapies that can persist and remain functional for months or years (Porter et al., 2015), allogeneic NK cells typically survive only a few weeks in the adoptive transfer setting (Geller et al., 2011; Miller et al., 2005). Therefore, engineering NK cells to improve their *in vivo* persistence would likely be beneficial to improve their anti-tumor activity. Human induced pluripotent stem cells (iPSCs) can be precisely genetically modified at a clonal level using both viral and non-viral methods and then efficiently differentiated to produce mature NK cells (iPSC-NK cells) (Knorr et al., 2013; Li et al., 2018). Therefore, iPSCs provide an important platform to produce human NK cells with improved anti-tumor activity (Li et al., 2018; Zhu et al., 2018, 2020). Indeed, previous studies have expressed novel NK cell-specific CARs that mediate improved killing of ovarian cancer cells *in vitro* and *in vivo* (Li et al., 2018). Additionally, stabilized expression of CD16 in iPSC-NK cells leads to improved antibody-dependent cell-mediated cytotoxicity (ADCC) and improved killing of both hematologic malignancies and solid tumors (Zhu et al., 2020).

Interleukin-15 (IL-15) stimulates multiple NK cell functions, including differentiation, proliferation, activation, and survival (Huntington et al., 2009; Ranson et al., 2003). In clinical trials,

IL-15 has been shown to stimulate NK cell proliferation and IL-15 levels correlated with *in vivo* expansion of infused NK cells in patients (Miller et al., 2018; Romee et al., 2018; Wrangle et al., 2018). However, high doses of IL-15 can cause toxicities (Flores and Tarhini, 2015; Miller et al., 2018). Therefore, increasing the sensitivity of NK cells to IL-15 to enable lower treatment doses of this cytokine provides an attractive approach to improve the anti-tumor activity of NK cells while eliminating the need for high doses of supplemental cytokines.

Cytokine-inducible SH2-containing protein (CIS) is the first member identified in the suppressor of cytokine signaling (SOCS) protein family (other members: SOCS 1–7) (Hilton et al., 1998). SOCSs are induced by cytokines and in turn inhibit cytokine signaling, forming a classic negative feedback loop (Delconte et al., 2016; Putz et al., 2017). All SOCS proteins contain the SOCS box sequence motif, which enables the SOCS proteins to function as adaptors for an E3 ubiquitin ligase complex and direct SOCS-interacting proteins to proteasomal degradation (Zhang et al., 2015). CIS, SOCS1, and SOCS3 have all been shown to bind directly to JAK1, inhibiting JAK-STAT signaling activation (Delconte et al., 2016; Kershaw et al., 2013). In mice, deletion of *Cish* augments IL-4 and IL-2 signaling in CD4⁺ T cells and increases sensitivity to IL-15 in NK cells, leading to better control of experimental tumor metastasis (Delconte et al., 2016; Putz et al., 2017). The same group showed that CIS might be important for human NK cell immunity by deletion of *CISH* in human primary NK cells (Rautela et al., 2018), although another group that used CRISPR-Cas-mediated knockout (KO) of *CISH* in primary human NK cells did not find improved anti-tumor activity (Pomeroy et al., 2018). *Cish* has also been reported to be induced by TCR stimulation in CD8⁺ T cells and inhibits their anti-tumor activity (Palmer et al., 2015). In humans, variants of *CISH* are associated with susceptibility to infectious diseases (Khor et al., 2010; Sun et al., 2014).

Cellular metabolism is now recognized to play a key role in regulating the function and differentiation of immune cells (Mah and Cooper, 2016; Marçais et al., 2017; O'Brien and Finlay, 2019; Pearce et al., 2013). Immune cells undergo dynamic metabolic shifts to support their activity, and recent studies have shown this is specifically true in the case of NK cell function (Gardiner, 2019; Kobayashi and Mattarollo, 2019; Poznanski and Ashkar, 2019; Wegiel et al., 2018). For example, interferon (IFN)- γ production via activating NK receptors requires glucose-driven oxidative phosphorylation (OxPhos) (Keppel et al., 2015). Another study showed that the mammalian target of rapamycin (mTOR) complex 1 (mTORC1), a key regulator of cellular metabolism, is robustly stimulated in activated NK cells and is required for the production of IFN- γ (Donnelly et al., 2014). Two separate groups demonstrated mTOR could be activated by IL-15 and is essential for IL-15-mediated NK cell proliferation during development and activation (Mao et al., 2016; Marçais et al., 2014). In addition, both aberrant glucose metabolism (Cong et al., 2018) and lipid accumulation (Michelet et al., 2018) in NK cells lead to dysfunction. However, there have been limited data showing that improving the metabolic fitness of NK cells mediates improved human NK cell function (Kobayashi and Mattarollo, 2019; Poznanski and Ashkar, 2019).

We hypothesized that deletion of *CISH* in human NK cells would improve their anti-tumor activities, similar to the approach

of blocking the critical immune checkpoints, such as PD-1 or CTLA-4. To test our hypothesis, we leveraged the iPSC-NK cell platform to knock out *CISH* in human NK cells at the clonal level. By utilizing iPSCs to derive gene-deleted NK cells, we ensure 100% of cells have the deleted gene, compared with studies that have used the CRISPR-Cas9 system to knock out genes in human PB-NK cells, which results in lower and more variable amounts of gene deletion and must be repeated with every donor cell population (Pomeroy et al., 2020). We demonstrate that *CISH*^{-/-} iPSC-NK cells have improved expansion, enhanced anti-tumor activity, and persistence *in vitro* and *in vivo*. Notably, deletion of *CISH* in human NK cells leads to augmented single-cell polyfunctionality, a profile that has been demonstrated to positively contribute to clinical outcome in CAR-T cells (Rossi et al., 2018). In addition, we show that *CISH*^{-/-} iPSC-NK cells exhibited improved metabolic fitness, which is mediated by the mTOR signaling pathway. More importantly, the increased metabolic fitness directly contributes to improved anti-tumor function in *CISH*^{-/-} iPSC-NK cells.

RESULTS AND DISCUSSION

Generation of *CISH*-KO NK Cells from Human iPSCs

Previous studies from our lab demonstrate that human iPSCs and human embryonic stem cells (hESCs) can be routinely differentiated into NK cells with phenotype and function similar to PB-NK cells (Knorr et al., 2013; Zhu and Kaufman, 2019). Here, we first examined CIS expression during different stages of NK cell differentiation. CIS expression was not detected in either undifferentiated iPSCs or early-stage hematopoietic progenitor cells (CD34⁺ cells isolated at day 6 of differentiation) (Figure S1A). However, CIS is induced by either IL-2 or IL-15 in iPSC-derived NK cells in a time-dependent manner, similar to PB-NK cells (Figures 1A and 1B).

iPSC provides a unique platform to do genetic modifications at the clonal level and then to derive large numbers (clinical scale) of genetically engineered NK cells produced from a standardized starting cell source (Knorr et al., 2013; Li et al., 2018; Zhu and Kaufman, 2019). To explore the role of CIS in human NK cells, we utilized this platform and knocked out *CISH* in human iPSCs by CRISPR-Cas9 technology (Figure 1C). We used a pair of guide RNAs (gRNAs) located in direct and complementary strand targeting exon 3 of the *CISH* gene right after the start codon (exon 2) (Figure 1C). This strategy was reported to enhance genome-editing specificity (Ran et al., 2013). We then selected 57 single clones and identified a *CISH*^{-/-} clone with frameshift mutations in both alleles (Figures 1D and 1E). All of the mutations were within the range of the gRNA targeting region. *CISH*^{-/-} iPSCs grow normally and maintain the typical phenotype and karyotype of undifferentiated iPSCs (Figures S1B–S1D), indicating CIS does not regulate the maintenance of undifferentiated human pluripotent stem cells. We then derived human *CISH*^{-/-} iPSC-NK cells from clonal *CISH*^{-/-} iPSCs and confirmed the loss of CIS expression in these cells by immunoblotting (Figure 1E).

CIS is an intracellular protein that negatively regulates IL-15 signaling and has been shown to be an important checkpoint to regulate NK cell-mediated anti-tumor immunity in mice (Delconte et al., 2016). These murine studies demonstrated that deletion of *Cish* rendered NK cells hypersensitive to IL-15, and

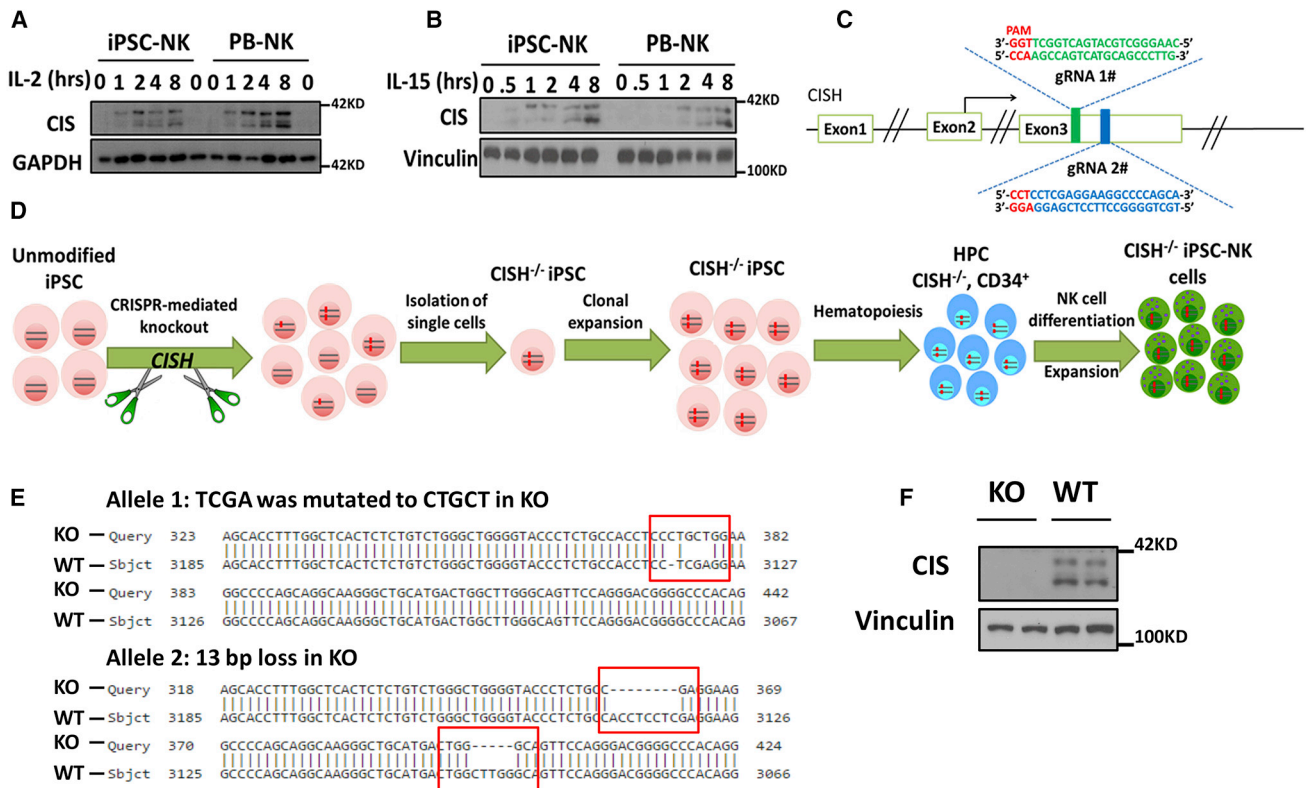


Figure 1. Generation of *CISH*-KO NK Cells from Human iPSCs

(A and B) To demonstrate normal CIS expression, we incubated iPSC-NK and PB-NK cells without cytokines for 8 h and then simulated with (A) 100 U/mL IL-2 or (B) 10 ng/mL IL-15 for the indicated times; then CIS expression was analyzed by immunoblotting (IB). GAPDH was used as loading control. (C) Schema of CRISPR-Cas9-mediated *CISH* KO using two guide RNAs (gRNA) located in direct and complementary strand targeting exon 3 of the *CISH* gene. (D) Schematic representation for deriving clonal *CISH*^{-/-} iPSC-NK cells from human iPSCs. CRISPR-Cas9-mediated *CISH* KO was performed in WT iPSCs, followed by identification of *CISH*^{-/-} iPSCs at clonal level. After clonal expansion, *CISH*^{-/-} iPSCs were differentiated to CD34⁺ hematopoietic progenitor cells through hematopoiesis and then *CISH*^{-/-} iPSC-NK cells through NK cell differentiation using the method previously reported. (E) Comparison of sequence in *CISH* KO clone (obtained by Sanger sequencing) with *CISH* WT sequence (exon 3, from 3,067 to 3,185) by Basic Local Alignment Search Tool (BLAST) showing frameshift mutations (red rectangles) in both alleles. All mutations occurred in two gRNA targeted regions. (F) WT iPSC-NK cells and *CISH*^{-/-} iPSC-NK cells were simulated with 10 ng/mL IL-15 for 8 h, and CIS expression was evaluated by IB. Vinculin was used as loading control.

Data in (A), (B), and (F) were repeated in three separate experiments.

Cish^{-/-} mice were resistant to multiple cancer metastases *in vivo* (Delconte et al., 2016). However, the impact of CIS on human NK cell function is less well defined. A key challenge preventing a better understanding of this protein's role in human NK cell biology has been establishing methodology to consistently and efficiently genetically modify human NK cells, especially when deleting intracellular components such as CIS. In this study, we used a well-defined system to produce homogeneous and well-characterized human iPSC-derived NK cells (Knorr et al., 2013; Li et al., 2018; Zhu and Kaufman, 2019).

Deletion of *CISH* in Human iPSCs Does Not Affect Hematopoiesis but Delays NK Cell Differentiation *In Vitro*

To investigate the role of CIS during hematopoietic development, we analyzed hematopoietic progenitor cell-surface antigens (CD31, CD34, CD43, and CD45) at day 6 of differentiation of wild type (WT) iPSCs and *CISH*^{-/-} iPSCs. The development

of hematopoietic progenitor cells was similar in both populations (~85% were CD34⁺CD31⁺ cells and ~40%–50% were CD34⁺CD43⁺) (Figures 2A and 2B), indicating loss of CIS does not affect early human hematopoietic differentiation. We then investigated the effect of deleting *CISH* during *in vitro* NK cell differentiation. After 3 weeks in NK cell differentiation conditions, WT iPSCs produced ~40% CD45⁺CD56⁺ NK cells; however, the *CISH*^{-/-} iPSCs produced only ~5% CD45⁺CD56⁺ NK cells at this early time point (Figure 2C). Although NK cell differentiation was typically fully complete with >90% CD45⁺CD56⁺ NK cells after 4 weeks using WT iPSCs, the *CISH*^{-/-} iPSC-cells produced only ~10% CD45⁺CD56⁺ NK cells at week 4 (Figure 2C). However, by week 5, these *CISH*^{-/-} iPSC-NK cell cultures contained >80% CD45⁺CD56⁺ NK cells (Figures 2C and 2D). Notably, the yields of NK cells produced by WT iPSCs and *CISH*^{-/-} iPSCs are comparable by week 5 (typically ~1 × 10⁷ CD45⁺CD56⁺ NK cells from 1 × 10⁶ starting iPSCs). These results demonstrate that deletion of CIS does lead to a

(Figure 2E). *CISH*^{-/-} iPSC-NK cells consist of a homogeneous population of CD56⁺ NK cells that co-express typical NK cell-surface antigens, including CD16, NKp44, NKp46, NKG2D, NKG2A, KIR, TRAIL, and FasL (Figure 2E), similar to WT iPSC-NK cells. In addition, *CISH*^{-/-} iPSC-NK cells and WT iPSC-NK cells similarly express NK cell maturation markers, such as CD94, CD2, CD57, and NKG2C (Figure 2E), indicating *CISH*^{-/-} iPSC-NK cells are phenotypically mature and *CISH* KO does not affect NK cell phenotype and maturation. To further characterize *CISH*^{-/-} iPSC-NK cells, we used mass cytometry (CyToF) and a panel of 37 antibodies against inhibitory, activating, and homing receptors, as well as intracellular activation markers (Table S1). As shown in the t-distributed stochastic neighbor-embedding (tSNE) algorithm map (Figure 2F), *CISH*^{-/-} iPSC-NK cells express typical NK cell-surface markers similar to WT iPSC-NK cells. Interestingly, some markers associated with NK cell, proliferation, and activation cytotoxicity are increased in *CISH*^{-/-} iPSC-NK cells, including Ki67, DNAM-1, 2B4, and Syk (Figures 2F and 2G). We then expanded *CISH*^{-/-} iPSC-NK cells using irradiated K562-IL21-4-1BBL cells and IL-2 as previously utilized by our group and others (Denman et al., 2012; Knorr et al., 2013). Under these culture and expansion conditions, *CISH*^{-/-} iPSC-NK cell expansion and cytolytic activity were similar to WT iPSC-NK cells (Figures S2A–S2C). In addition, degranulation and cytokine production (Figure S2D) upon stimulation are similar among WT iPSC-NK, *CISH*^{-/-} iPSC-NK, and PB-NK cells under these culture and expansion conditions. Taken together, these data demonstrate that *CISH*^{-/-} iPSC-NK cells are phenotypically mature and have normal proliferative capacity under highly stimulated culture conditions.

***CISH*^{-/-} iPSC-NK Cells Display Better Expansion and Function Compared with WT iPSC-NK Cells under Low Cytokine Concentration**

Due to the role of CIS in inhibiting IL-15-mediated NK functions, we hypothesized that *CISH*^{-/-} iPSC-NK cells may have better expansion and function under “stimulus-lacking” (IL-15-limiting) conditions. We therefore maintained WT iPSC-NK cells and *CISH*^{-/-} iPSC-NK cells either without cytokines or at a low concentration of IL-15 (1 ng/mL, compared with the normal 10 ng/mL IL-15 conditions) (Felices et al., 2018; Wagner et al., 2017) for 3 weeks. WT iPSC-NK cells were unable to survive when maintained at the low concentration of IL-15 or without cytokines (Figures 3A and 3B). In contrast, *CISH*^{-/-} iPSC NK cells were able to expand for 3 weeks (>10-fold expansion) at the low concentration of IL-15 (Figure 3A). Similar findings were observed using a low concentration of IL-2 (10 U/mL, compared with the normal 50–100 U/mL) (Knorr et al., 2013; Li et al., 2018; Wagner et al., 2017) (Figure 3B). We then evaluated anti-tumor activity using cytotoxicity assays against K562, MOLM-13 (two myeloid leukemia lines), and SKOV-3 (ovarian cancer line). Notably, after culturing with 1 ng/mL IL-15 for 3 weeks, *CISH*^{-/-} iPSC NK cells still maintained potent anti-tumor activity and exhibited better killing activity against tumor targets in both short-term (4 h) and long-term (>20 h) cytotoxicity assays than WT iPSC-NK cells (Figures 3C–3F). Furthermore, we used NK cell degranulation (indicated by cell-surface expression of CD107a) and IFN- γ expression as parameters for NK cell function. Consistent with cytotoxicity results, WT iPSC-NK cells expressed minimal

amounts of both CD107a and IFN- γ when stimulated with the tumor cells, indicating loss of function when cultured long term with a low concentration of cytokine (Figures 3G–3I). In contrast, *CISH*^{-/-} iPSC NK cells exhibited significantly increased cytotoxic granule release (CD107a expression) and IFN- γ production (Figures 3G–3I) when stimulated. To further extend this finding, we cultured WT iPSC-NK, *CISH*^{-/-} iPSC NK, and PB-NK cells from two donors (PB-NK-1# and PB-NK-2#) with either low concentration of IL-15 (1 ng/mL) or normal concentration of IL-15 (10 ng/mL) for 3 and 7 days, and evaluated their killing activity against K562 cells (Figure S3). After culture with low IL-15 for 7 days, *CISH*^{-/-} iPSC NK cells show better killing activity compared with WT iPSC-NK or PB-NK cells (Figure S3B). However, no significant difference in killing activity was observed when cultured with normal IL-15 for 3 and 7 days (Figures S3C and S3D). Together, these results demonstrate that deletion of *CISH* in NK cells leads to improved survival and function when cytokine stimulation is limiting.

CISH*^{-/-} iPSC-NK Cells Display Improved Anti-tumor Activity *In Vivo

To evaluate the anti-tumor activity of *CISH*^{-/-} iPSC-NK cells *in vivo*, we assessed their killing of MOLM-13 AML cells in a mouse xenograft tumor model. Mice were injected intravenously (i.v.) with luciferase-expressing MOLM-13 cells and the next day received a single i.v. injection of 1×10^7 WT or *CISH*^{-/-} iPSC-NK cells (Figure 4A). As in previous studies (Li et al., 2018), IL-2 was dosed every other day for 21 days to promote *in vivo* NK cell survival and expansion. Tumor growth was monitored by bioluminescent imaging (BLI) (Figure 4B). Treatment with NK cells significantly reduced tumor burden, and *CISH*^{-/-} iPSC-NK cells mediated significantly better anti-tumor activity when compared with treatment using WT iPSC-NK cells (Figures 4B and 4C). This led to markedly improved survival of mice treated with the *CISH*^{-/-} iPSC-NK cells. Three out of five mice treated with *CISH*^{-/-} iPSC-NK cells had complete tumor clearance and long-term (>100 days) survival versus zero of five mice treated with WT iPSC-NK cells (Figure 4D). Moreover, we investigated the *in vivo* persistence of NK cells by examining peripheral blood for the presence of human NK cells (hCD56⁺ cells). On day 7, the number of *CISH*^{-/-} iPSC-NK cells was significantly higher (38.2 ± 4.3 compared with 12.0 ± 2.8 cells/ μ L; $p < 0.001$) in circulation than in WT iPSC-NK cells (Figures 4E and 4F). Next, we performed a separate study to compare the *in vivo* persistence and homing of WT iPSC-NK cells, *CISH*^{-/-} iPSC-NK cells, and PB-NK cells (Figure S4). Again, *CISH*^{-/-} iPSC-NK cells show significantly better persistence in peripheral blood in comparison with WT iPSC-NK cells or PB-NK cells at day 7 (Figures S4A and S4B). Moreover, at day 14, *CISH*^{-/-} iPSC-NK cells exhibited better persistence in peripheral blood, spleen, and homing to bone marrow (Figures S4C–S4F). Together, these studies demonstrate that *CISH*^{-/-} iPSC-NK cells have improved anti-tumor activity and persistence *in vivo*.

***CISH*^{-/-} iPSC-NK Cells Show Increased IL-15 Signaling Activation**

To further investigate the molecular mechanisms that mediate improved function of *CISH*^{-/-} iPSC-NK cells, we performed RNA sequencing on WT iPSC-NK cells and *CISH*^{-/-} iPSC-NK

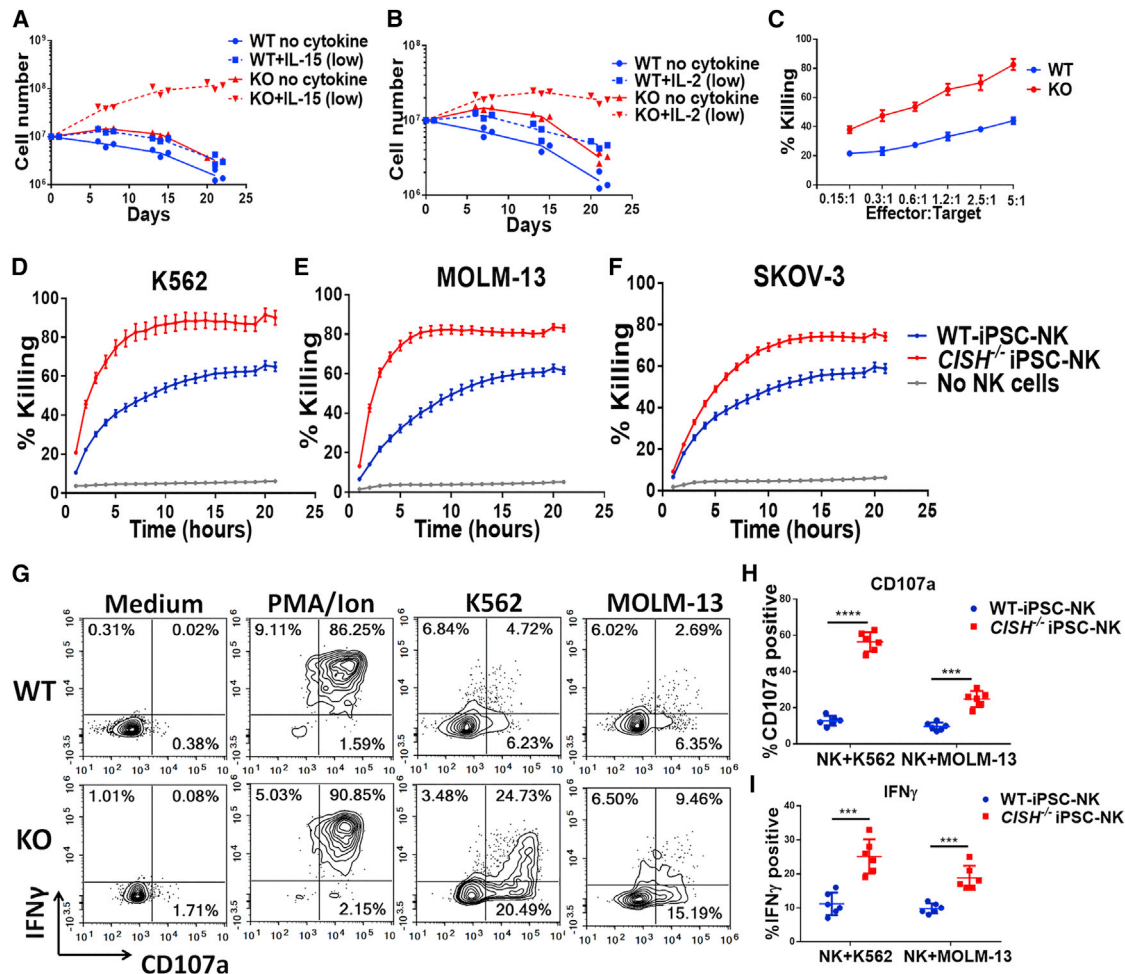


Figure 3. *CISH*^{-/-} iPSC-NK Cells Have Better Expansion and Functions *In Vitro* Compared with WT iPSC-NK Cells

(A and B) Growth curve of *CISH*^{-/-} iPSC-NK cells and WT iPSC-NK cells with or without a low concentration of (A) IL-15 (1 ng/mL) and (B) IL-2 (10 U/mL). Data were repeated independently in three separate experiments.

(C) Four-hour cytotoxicity assay using *CISH*^{-/-} iPSC-NK and WT iPSC-NK cells against K562 cells after 3 weeks of culture in low-concentration IL-15 as determined using CellEvent Caspase-3/7 Green Flow Cytometry Assay.

(D–F) Killing against K562 (D), MOLM-13 (E), and SKOV-3 (F) cells was quantified over an extended time course using the IncuCyte real-time imaging system at effector-to-target (E:T) = 1:1.

(G) *CISH*^{-/-} iPSC-NK cells and WT iPSC-NK cells were maintained at low IL-15 for 3 weeks, and production of CD107α and IFN-γ in response to K562 and MOLM-13 cells was measured. *CISH*^{-/-} iPSC-NK cells and WT iPSC-NK cells were left unstimulated or stimulated with a 1:1 ratio of target cells and stained for CD107α and IFN-γ 4 h later.

(H and I) Quantification of CD107α (H) (n = 6) and IFN-γ (I) (n = 6) after stimulation with K562 or MOLM-13 cells. Paired t test was used to do the comparisons. ***p < 0.001, ****p < 0.0001.

(C–F, H, and I) Data were shown as mean ± SD. (C–I) Data were repeated in three separate experiments.

cells. Surprisingly, more than 6,000 differentially expressed genes (the threshold of differential expression genes is p value adjusted (padj) < 0.05) were identified in *CISH*^{-/-} iPSC-NK cells (Figure 5A). Gene ontology (GO) enrichment analysis suggested that the top upregulated signaling pathways in *CISH*^{-/-} iPSC-NK cells were associated with leukocyte differentiation, proliferation, activation, and cytokine secretion (Figure 5B; Table S2). These findings confirmed a role for *CIS* to regulate NK cell differentiation, and this finding is consistent with our data that deletion of *CISH* delayed NK cell *in vitro* differentiation. Notably, more than 60 genes involved in positive regulation of lymphocyte activation were significantly upregulated in *CISH*^{-/-} iPSC-NK cells

compared with WT iPSC-NK cells (Figure 5C). We next analyzed IL-15 signaling in *CISH*^{-/-} iPSC-NK cells. Kyoto Encyclopedia of Genes and Genome (KEGG) analysis of RNA sequencing data showed that the JAK-STAT pathway (IL-15 downstream pathway) is one of the most upregulated signaling pathways in *CISH*^{-/-} iPSC-NK cells (Figure 5D). Expression of 34 genes involved in the JAK-STAT signaling pathway was significantly upregulated in *CISH*^{-/-} iPSC-NK cells compared with WT iPSC-NK cells (Figure 5D). More specific analysis of cell signaling pathways demonstrated markedly increased phosphorylation of IL-15-stimulated JAK1 tyrosine phosphorylation, STAT3, and STAT5 in *CISH*^{-/-} iPSC-NK cells (Figure 5E). mTOR signaling

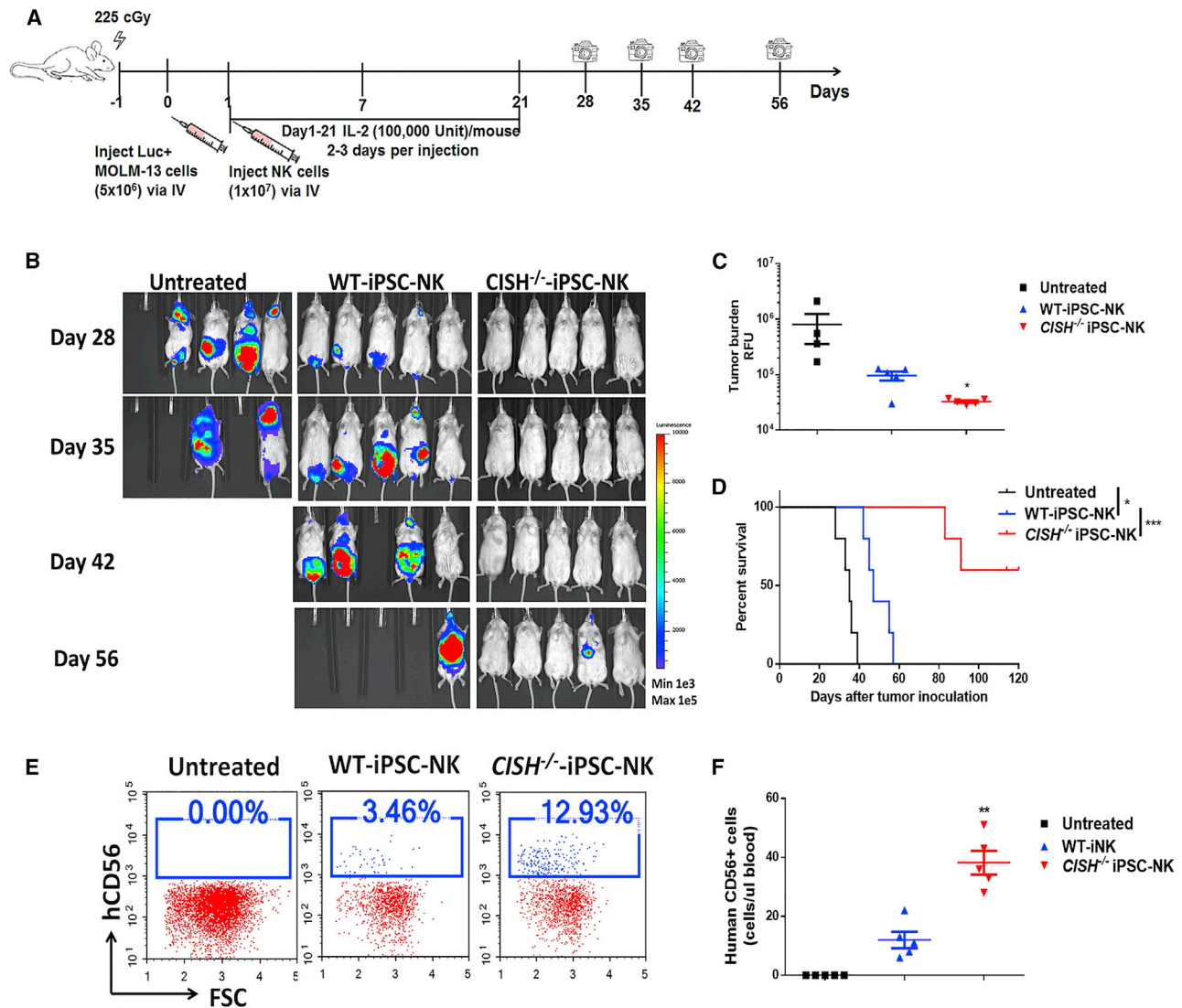


Figure 4. *CISH*^{-/-} iPSC-NK Cells Demonstrate Improved Persistence and Better Anti-tumor Activity *In Vivo*

(A) Diagram of *in vivo* treatment scheme. Non-obese diabetic/severe combined immunodeficiency/ γ c^{-/-} (NSG) mice were inoculated i.v. with 5×10^6 MOLM-13 cells expressing the firefly luciferase gene. One day after tumor injection, mice were either left untreated or treated with 1×10^7 WT iPSC-NK or *CISH*^{-/-} iPSC-NK cells. NK cells were supported by weekly injections of IL-2 for 3 weeks, and IVIS (In Vivo Image System) imaging was done to track tumor load.

(B) IVIS images showing progression of tumor burden.

(C) Tumor burden at day 28 was quantified and shown as mean \pm SD. Statistics by one-way ANOVA test; * $p < 0.05$.

(D) Kaplan-Meier curve demonstrating survival of the experimental groups. Statistics: two-tailed log rank test, WT iPSC-NK versus untreated, * $p < 0.05$; WT iPSC-NK versus *CISH*^{-/-} iPSC-NK, *** $p < 0.001$.

(E) Representative flow cytometry plot of human CD56⁺ cells in population from mouse peripheral blood 7 days after NK cell treatment.

(F) Quantification of human CD56⁺ cells in peripheral blood (number of hCD56⁺ cells/ μ L blood) at day 7, shown as mean \pm SD. Statistics by one-way ANOVA test; ** $p < 0.01$.

activity, which can be stimulated by IL-15 in NK cells (ref), is also upregulated in *CISH*^{-/-} iPSC-NK cells as indicated by an increased level of phosphorylated S6 (p-S6) and phosphorylated S6K1 (p-S6K1) (Figure 5F). Expression of CD122, a subunit shared by the receptors for IL-2 and IL-15, was also increased in *CISH*^{-/-} iPSC-NK cells with or without IL-15 stimulation (Figures 5G and 5H). This increase in expression contributes to the increase in IL-15 signaling. IL-15 stimulation leads to downregulation of CD122 in both WT and *CISH*^{-/-} iPSC NK cells (Figures

5G and 5H). Together, these data suggest that increased expression of genes involved in the lymphocyte and IL-15 signaling activation pathways in *CISH*^{-/-} iPSC-NK cells provides a molecular mechanism for enhanced NK cell function.

***CISH*^{-/-} iPSC-NK Cells Show Increased Single-Cell Polyfunctionality**

A recent study identified a subset of polyfunctional T cells in CAR-T cell products that produce ≥ 2 cytokines upon

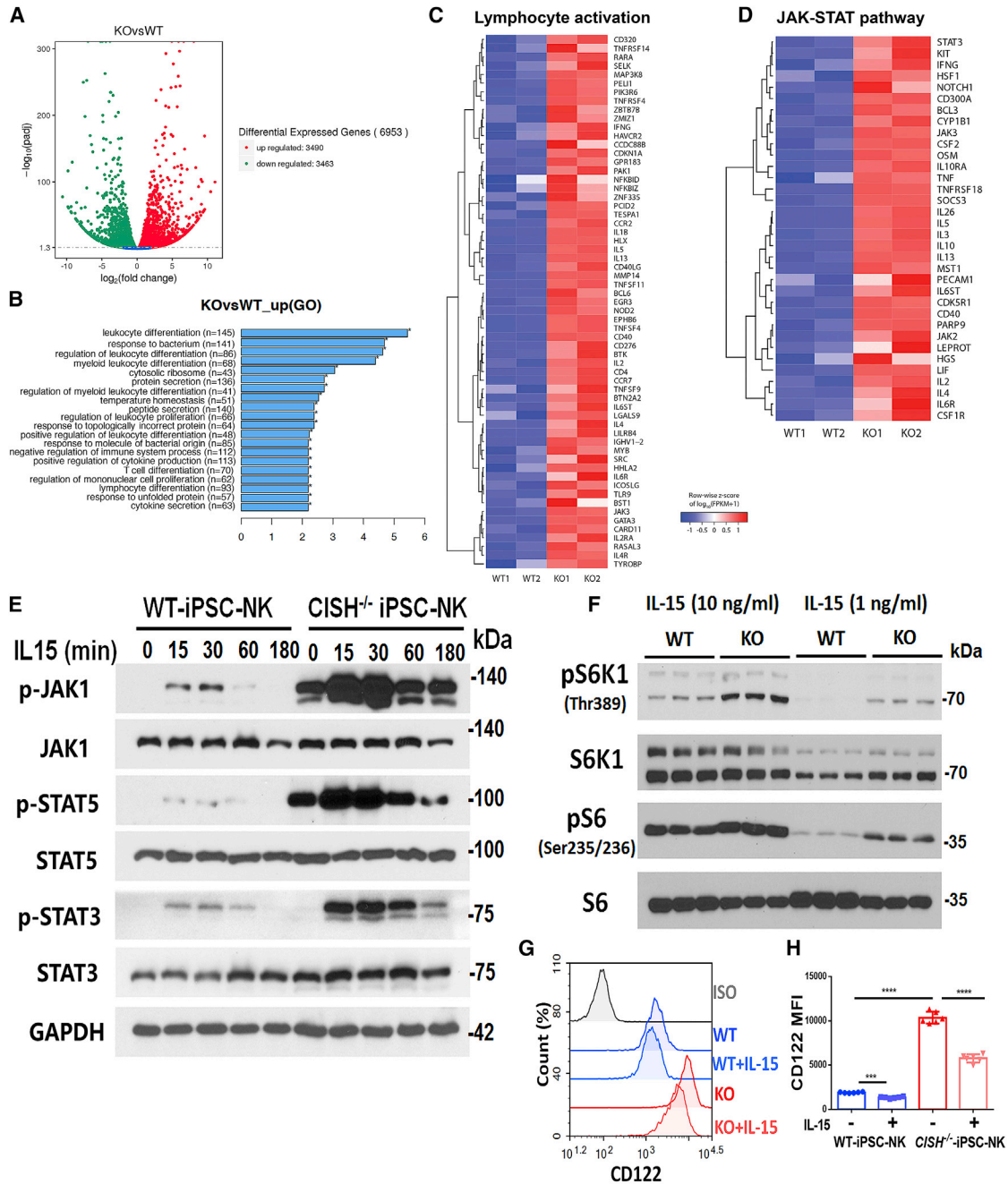


Figure 5. *CISH*^{-/-} iPSC-NK Cells Show Increased IL-15 Signal Activation

(A–D) Differential expression gene between WT iPSC-NK and *CISH*^{-/-} iPSC-NK cells was analyzed by RNA sequencing. (A) Volcano diagram of differential expression genes. The threshold of differential expression genes is padj < 0.05. (B) Gene ontology (GO) analysis of significantly enriched genes in *CISH*^{-/-} iPSC-NK cells. Bar charts show the top 20 significantly enriched GO terms for molecular function, biological process, and cellular components in *CISH*^{-/-} iPSC-NK cells. (C) Heatmap view of expression of 61 genes involved in regulating lymphocyte activations in WT iPSC-NK and *CISH*^{-/-} iPSC-NK cells. (D) Heatmap view of the JAK-STAT pathway gene expression in WT iPSC-NK and *CISH*^{-/-} iPSC-NK cells.

(E) IB analysis of WT iPSC-NK and *CISH*^{-/-} iPSC-NK cells incubated without cytokines for 24 h and then simulated with 1 ng/mL IL-15 for the indicated times. (F) IB analysis of mTOR downstream activation (pS6 and pS6K1) in WT iPSC-NK and *CISH*^{-/-} iPSC-NK cells cultured in media with 10 or 1 ng/mL IL-15 for 24 h. (G) Representative flow cytometry plot of IL-2R β (CD122) surface expression on WT iPSC-NK and *CISH*^{-/-} iPSC-NK cells cultured in media with or without IL-15 (1 ng/mL) for 24 h.

(H) Quantification of CD122 expression (n = 6).

Statistics: one-way ANOVA, ***p = 0.0002, ****p < 0.0001. Data at (E), (G), and (H) were repeated in three separate experiments, and data at (F) were repeated in two separate experiments. MFI, mean fluorescence intensity.

stimulation with CD19 antigen using high-content single-cell multiplex cytokine analysis (Rossi et al., 2018). Notably, pre-specified polyfunctionality strength index (PSI)-manufactured CAR-T cells were associated with improved clinical responses and reduced toxicities in non-Hodgkin's lymphoma patients (Rossi et al., 2018; Xue et al., 2017). Given the key role of IL-15 to regulate NK cell expansion and functionality, we examined whether the increase in IL-15 signaling activation in *CISH*^{-/-}-iPSC-NK cells similarly led to increased single-cell polyfunctional profiles, thus contributing to increased cytotoxicity of these cells. We evaluated polyfunctionality of *CISH*^{-/-}-iPSC-NK cells, WT iPSC-NK cells, and PB-NK cells (from two donors) using the same high-content single-cell multiplex cytokine analysis used in the CAR-T cell studies (Rossi et al., 2018; Xue et al., 2017). Cells were incubated at a low concentration of IL-15 (1 ng/mL) overnight and then simulated with IL-12 (10 ng/mL)/IL-18 (100 ng/mL) to elicit cytokine production. The polyfunctional profile of iPSC-NK cells and PB-NK cells upon stimulation with IL-12/IL-18 was dominated by effector molecules, including granzyme B, IFN- γ , Macrophage Inflammatory Protein 1 α (MIP-1 α), Perforin, and tumor necrosis factor alpha (TNF- α) (Figure S5). Notably, *CISH*^{-/-}-iPSC-NK cells showed the highest polyfunctional response with approximately 5% of total cells (~25% of all cytokine-producing NK cells) being polyfunctional, whereas only about 1%–2% of the WT iPSC-NK cells and PB-NK cells were polyfunctional (Figure S5). Moreover, the PSI was increased >10-fold in *CISH*^{-/-}-iPSC-NK cells compared with WT iPSC-NK cells and PB-NK cells. These results demonstrate that *CISH*^{-/-}-iPSC-NK cells have better single-cell polyfunctionality in comparison with WT iPSC-NK and PB-NK cells.

Deletion of *CISH* in Human iPSC-NK Cells Improves Metabolic Fitness

Activated NK cells upregulate the rate of glucose-driven glycolysis and OxPhos to provide energy to drive the pathways necessary for their effector functions (Kobayashi and Mattarollo, 2019; Mah and Cooper, 2016). Because IL-15 can exert important effects on NK cell metabolism (Felices et al., 2018; Marçais et al., 2014), we compared the glycolytic and mitochondrial function of WT iPSC-NK, *CISH*^{-/-} iPSC-NK, and PB-NK cells after incubation with a low concentration of IL-15 for 3 and 7 days using previously described Seahorse assays (Felices et al., 2018). Interestingly, after 3-day culture in low IL-15, the glycolytic rate was slightly increased in *CISH*^{-/-} iPSC-NK cells in comparison with both WT iPSC-NK and PB-NK cells, which was reflected through an increase in basal glycolysis (measured before the addition of rotenone/antimycin A) (Figures 6A and 6B) and an increase in glycolytic capacity elucidated by subtracting the rate of glycolysis before and after addition of 2-deoxy-D-glucose (2DG) (Figures 6A and 6B). After 3-day culture in low IL-15, OxPhos was also increased in *CISH*^{-/-} iPSC-NK cells compared with WT iPSC-NK and PB-NK cells (Figure 6C). Maximal respiration was significantly increased in *CISH*^{-/-} iPSC-NK cells compared with WT iPSC-NK and PB-NK cells (Figure 6D). ATP-linked respiration, which was calculated from subtraction of basal respiration and respiration after addition of oligomycin, and mitochondrial spare respiratory capacity (SRC) measured after addition of carbonyl cyanide-4-(trifluoromethoxy) phenylhydrazone (FCCP) were modestly increased or

showed a trend of increase in *CISH*^{-/-} iPSC-NK cells (Figure 6D). Although after 7-day culture with low IL-15, both glycolytic rate (Figures 6E and 6F) and OxPhos (Figures 6G and 6H) were dramatically increased in *CISH*^{-/-} iPSC-NK cells compared with WT iPSC-NK and PB-NK cells.

Glucose-driven glycolysis and oxidative metabolism have been shown to be required for NK cell anti-tumor and anti-viral effector functions (Assmann et al., 2017; Donnelly et al., 2014; Keppel et al., 2015; Poznanski and Ashkar, 2019). This suggests that the increased IFN- γ production and cytotoxic activity of *CISH*^{-/-} iPSC-NK cells were supported by increased glycolysis and OxPhos. Notably, SRC has been shown to be pivotal in memory T cell formation and could be used as an indicator of metabolic fitness (Pearce et al., 2013). These data demonstrate that *CISH*^{-/-} iPSC-NK cells have improved metabolic fitness that can mediate potentially enhanced functions.

Improved Metabolic Fitness in *CISH*^{-/-} iPSC-NK Cells Is Mediated by mTOR Signaling and Contributes to Enhanced Function

Although the importance of cellular metabolism on immune cell function is now well established, there have been more limited data on the ability to improve or optimize human NK cell-mediated activity via improved metabolic fitness of NK cells (Kobayashi and Mattarollo, 2019). We therefore tested whether improved metabolic fitness in *CISH*^{-/-} iPSC-NK cells contributes to enhanced cytotoxicity. We used rapamycin (rapa), an inhibitor of mTORC1 and key regulator of cellular metabolism (Donnelly et al., 2014; Marçais et al., 2014). rapa treatment decreased proliferation of both *CISH*^{-/-} iPSC-NK and WT iPSC NK cells (Figure 7A). Interestingly, treatment of *CISH*^{-/-} iPSC-NK cells with rapa led to both decreased glycolysis and mitochondrial respiration (Figures 7B–7E). rapa completely neutralized the improved glycolysis and OxPhos in *CISH*^{-/-} iPSC-NK cells, bringing the metabolic rate to a level similar to WT iPSC-NK cells (Figures 7B–7E). Notably, rapa did not affect either glycolysis or mitochondrial respiration of WT iPSC-NK cells (Figures 7B–7E). Indeed, treating with rapa slightly increased the ATP-linked aspiration rate in WT iPSC-NK cells (Figure 7E). This indicates that the metabolic rate in WT iPSC-NK cells under low cytokine concentration is reduced to a level that could not be further decreased by inhibition of mTOR signaling.

To investigate whether improved metabolic fitness in *CISH*^{-/-} iPSC-NK cells directly contributes to enhanced cytotoxicity, we evaluated cytotoxicity after treatment with rapa. rapa-mediated decrease of glycolysis and mitochondrial respiration in *CISH*^{-/-} iPSC-NK cells resulted in decreased cytotoxicity (Figure 7F), degranulation (Figures 7G and 7H), and cytokine production (Figures 7G and 7I). These results demonstrate that the improved metabolic fitness in *CISH*^{-/-} iPSC-NK cells is mediated by the mTOR pathway and directly contributes to enhanced NK cell functions.

Using human stem cell-derived NK cell as a platform, we demonstrated that deletion of *CIS* in NK cells increased IL-15-mediated JAK-STAT pathway signaling activity, similar to their functions in mouse. We further demonstrated that human *CISH*^{-/-} NK cells exhibited improved mTOR-mediated metabolic fitness, which directly contributes to the improved anti-

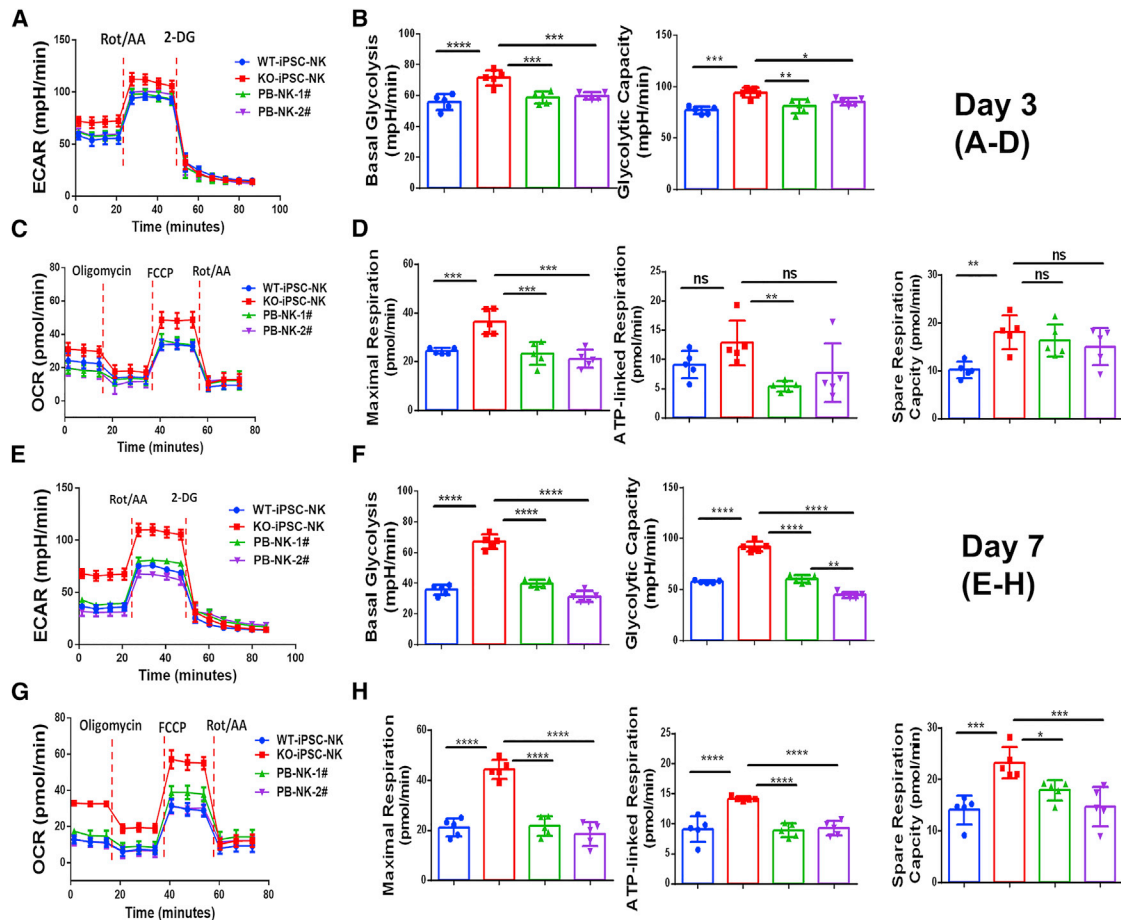


Figure 6. Deletion of *CISH* in Human iPSC-NK Cells Improves Metabolic Fitness

WT iPSC-NK, *CISH*^{-/-} iPSC-NK, and PB-NK cells from two donors (PB-NK-1# and PB-NK-2#) were incubated with a low concentration of IL-15 (1 ng/mL) for 3 (A–D) or 7 days (E–H).

(A) The extracellular acidification rate (ECAR) was measured in real time in an XFe96 analyzer after injection of rotenone/antimycin A (Rot/AA) and 2-deoxy-D-glucose (2DG).

(B) Graphical analysis of basal glycolysis (left) and glycolytic capacity (right) derived from (A) (n = 6).

(C) The oxygen consumption rate (OCR) was measured after injection of oligomycin, carbonyl cyanide-4-(trifluoromethoxy) phenylhydrazone (FCCP), and Rot/AA.

(D) Graphical analysis of maximal respiration (left), ATP-linked respiration (middle), and spare respiration capacity (SRC, right) derived from (C) (n = 6).

(E) ECAR was measured.

(F) Graphical analysis of basal glycolysis (left) and glycolytic capacity (right) derived from (E) (n = 6).

(G) OCR was measured.

(H) Graphical analysis of maximal respiration (left), ATP-linked respiration (middle), and SRC (right) derived from (G) (n = 6).

Data were shown as mean ± SD and were repeated in three separate experiments. One-way ANOVA was used to do all comparisons. **p < 0.01, ***p < 0.001, ****p < 0.0001, ns p > 0.05.

tumor activity. Furthermore, we showed that deletion of *CISH* dramatically increases *in vivo* persistence of NK cells after adoptive transfer, as well as improved single-cell polyfunctionality measured by production of multiple effector cytokines that might also contribute to their improved anti-tumor functions.

Cellular metabolism is now recognized to play a key role regulating the function and differentiation of immune cells (Gardiner, 2019; O'Brien and Finlay, 2019; Pearce et al., 2013). Immune cells undergo dynamic metabolic shifts to support their activity, including overcoming the suppressive tumor microenvironment (TME) that changes the metabolism of immune cells, a process that inhibits the activity of these cells (Wegiel et al., 2018). The metabolic profile of CAR-T cells is known to play a key role in their

in vivo proliferation and function (Kawalekar et al., 2016). Multiple studies show that metabolic activity also regulates the cytolytic ability of NK cells (Gardiner, 2019; Kobayashi and Mattarollo, 2019; O'Brien and Finlay, 2019; Poznanski and Ashkar, 2019). Therefore, identifying key cellular and molecular mechanisms that regulate immune cell metabolism provides an important strategy to engineer immune cells to overcome the immune-suppressive TME. IL-15 can regulate NK cell metabolism, but its effects are complicated and controversial, depending on time and dose. Treating NK cells with high-dose IL-15 (100 ng/mL) for 72 h increases both glycolysis and OxPhos (Marçais et al., 2014). Notably, continuous treatment of NK cells with IL-15 (10 ng/mL) for 9 days led to NK cell exhaustion, impaired metabolism,

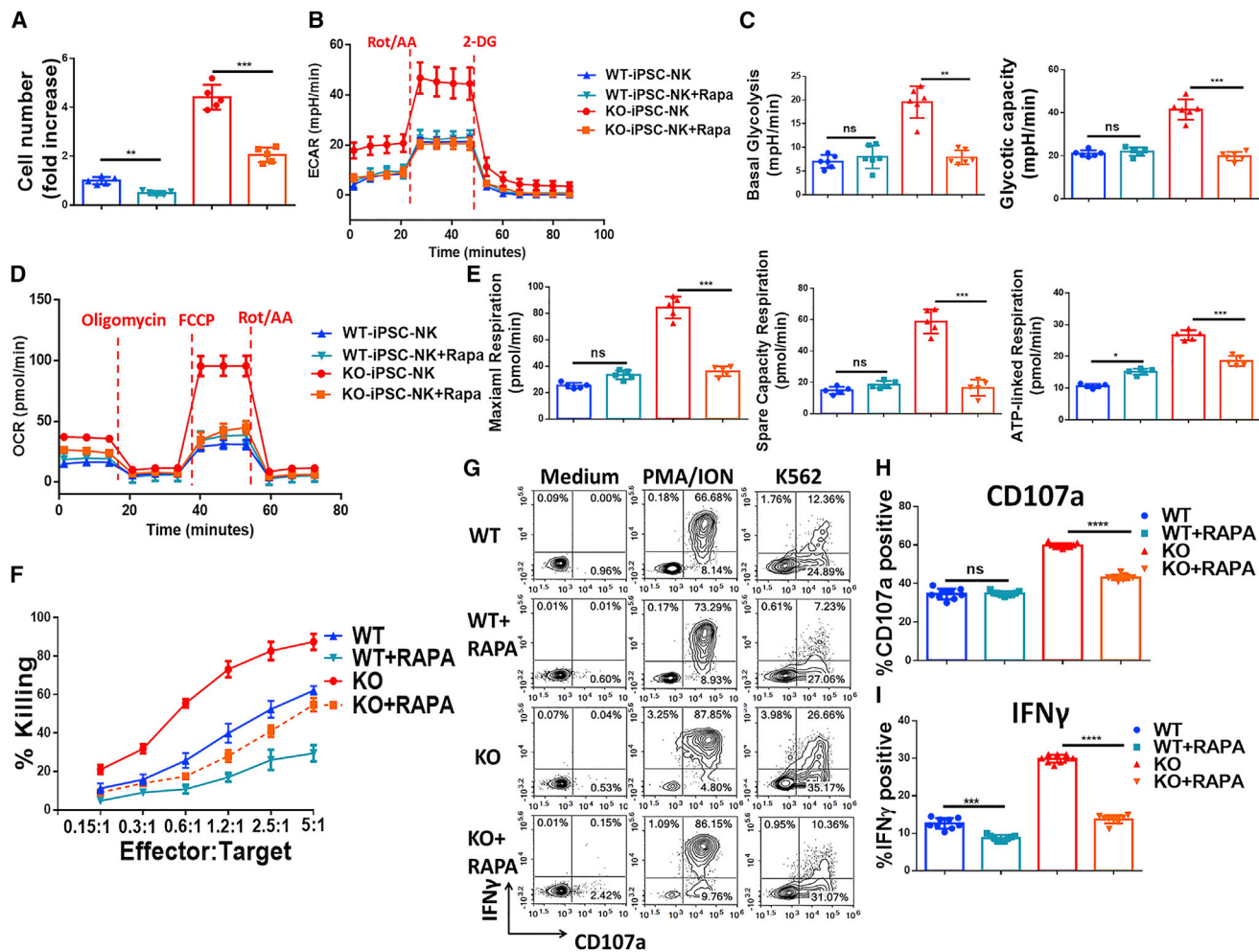


Figure 7. Improved Metabolic Fitness in *CISH*^{-/-} iPSC-NK Cells Is Mediated by the mTOR Signaling Pathway and Contributes to Improved Function

WT iPSC-NK and *CISH*^{-/-} iPSC-NK cells were incubated at a low concentration of IL-15 (1 ng/mL) with or without rapamycin (100 ng/mL) for 7 days.

(A) Quantification of rapamycin's effects upon NK cell proliferation.

(B) Rapamycin decreases the ECAR of *CISH*^{-/-} iPSC-NK cells to a level similar to that observed in WT iPSC-NK cells regardless of rapamycin's addition. ECAR was measured in real time in an XFe96 analyzer after injection of Rot/AA and 2-DG.

(C) Graphical analysis of basal glycolysis (left) and glycolytic capacity (right) derived from (B) (n = 6).

(D) OCR was measured after injection of oligomycin, FCCP, and Rot/AA.

(E) Graphical analysis of maximal respiration (left), SRC (middle), and ATP-linked respiration (right) derived from (D) (n = 6).

(F) After 7-day incubation with or without rapamycin, killing against K562 cells was evaluated using CellEvent Caspase-3/7 Green Flow Cytometry Assay.

(G) *CISH*^{-/-} iPSC-NK and WT iPSC-NK cells produce CD107a and IFN- γ in response to K562 with or without rapamycin for 7 days (low-dose IL-15, 1 ng/mL). *CISH*^{-/-} iPSC-NK and WT iPSC-NK cells were left unstimulated or stimulated with a 1:1 ratio of target cells and stained for CD107a and IFN- γ 4 h later.

(H and I) Quantification of CD107a (H) (n = 6) and IFN- γ (I) (n = 6) after stimulation with K562 or MOLM-13 cells. Data were shown as mean \pm SD and were repeated in three separate experiments. Paired t test was used to do all comparisons. *p < 0.05, **p < 0.01, ***p < 0.001, ****p < 0.0001.

and reduced cytotoxicity (Felices et al., 2018). The same group reported that human adaptive NK cells (CD3⁺CD56^{dim}CD57⁺NKG2C⁺) exhibited increased mitochondrial respiration, which contributes to the increased IFN- γ production in these cells (Cichocki et al., 2018). Here, we increased sensitivity of NK cells to IL-15 stimulation by removing a negative regulator, CIS. When challenged with an extremely low concentration of IL-15 (1 ng/mL), which is 10 times lower than the normal concentration (Felices et al., 2018; Wagner et al., 2017), for up to 3 weeks, *CISH*^{-/-} iPSC-NK cells exhibited increased expansion and improved function, which we attributed to improved metabolic

fitness in comparison with WT iPSC-NK cells. These results show that long-term administration of IL-15 can be beneficial to NK cell metabolism and, therefore, function when the dose is optimized and attenuated. Cryopreservation is key for developing off-the-shelf cell therapy products. Recent studies indicated that metabolic pathways play a key role in the cell cryopreservation process (Fu et al., 2019), and IL-15-activated cytokine-induced killer (CIK) cells were able to maintain phenotype and cytotoxicity potential after long-term cryopreservation (Bremm et al., 2019). Whether knocking out *CISH* can improve cryopreservation of NK cells needs further investigations.

These studies demonstrate that CIS is a key regulator of human NK cell survival and anti-tumor activity. Deletion of CIS does not affect *in vitro* maintenance of undifferentiated human iPSCs and hematopoietic differentiation but delays *in vitro* NK cell differentiation. *CISH*^{-/-} iPSC-NK cells have an improved metabolic profile and exhibit increased expansion and enhanced cytotoxicity when maintained at a low concentration of IL-15 *in vitro*. When tested in a human AML xenograft tumor model, *CISH*^{-/-} iPSC-NK cells exhibited improved *in vivo* persistence and anti-tumor activities in comparison with WT iPSC-NK cells. Mechanistically, we found that the enhanced anti-tumor function could be attributed to the increased single-cell polyfunctionality and mTOR-mediated metabolic fitness.

Recent advances in NK cell-based adoptive immunotherapy, including the development of novel NK cell-specific CARs to enhance iPSC-derived NK cell-targeted anti-tumor activity (Li et al., 2018) and stabilizing CD16 expression to boost ADCC, have yielded some exciting results (Zhu et al., 2020). These experimental studies are being translated into clinical therapies with iPSC-derived NK cells now in clinical trials for treatment of refractory malignancies (ClinicalTrials.gov: NCT03841110 and NCT04023071). These phase 1 trials include use of un-engineered iPSC-derived NK cells combined with checkpoint inhibitors for treatment of refractory solid tumors, as well as iPSC-derived NK cells engineered to express a non-cleavable, high-affinity CD16 to mediate improved ADCC (Zhu et al., 2018, 2020). A trial using iPSC-NK cells that express an NK cell-specific CAR is also planned (Li et al., 2018). Together, this advancement of iPSC-derived NK cells into clinical trials highlights the ability for iPSCs to provide a unique platform to create NK cells with one or multiple genetic modifications (such as combination of CIS-deletion and CAR modification) to produce NK cells with improved metabolic fitness and enhanced anti-tumor functions (Zhu et al., 2018).

In summary, we report that silencing of an intracellular immune checkpoint in NK cells increases their single-cell polyfunctionality and improves their metabolic fitness, leading to enhanced functions. These studies support clinical validation of blocking this intracellular immune checkpoint and improving metabolic fitness to enhance NK cell-mediated anti-tumor activities for adoptive immunotherapy. We believe that metabolic and cytokine response reprogramming through *CISH* KO can be combined with other exciting advances in NK cell immunotherapy, including tumor target recognition (CAR and hnCD16) and immune checkpoint blockade, among others, to produce an all-in-one NK cell product for next generation immunotherapy.

STAR★METHODS

Detailed methods are provided in the online version of this paper and include the following:

- KEY RESOURCES TABLE
- RESOURCE AVAILABILITY
 - Lead Contact
 - Materials Availability
 - Data and Code Availability

● EXPERIMENTAL MODEL AND SUBJECT DETAILS

- Mouse Strain
- Cells

● METHOD DETAILS

- Cell culture
- Generation, identification and karyotyping of clonal *CISH*^{-/-} iPSC
- Derivation and expansion of NK cells from WT and *CISH*^{-/-} iPSCs
- Isolation and expansion of PB-NK cells
- Immunoblotting
- Flow cytometry
- Mass cytometry
- CD107a expression and IFN- γ staining
- CellEvent Caspase-3/7 Green Flow Cytometry assay
- IncuCyte Caspase-3/7 Green Apoptosis assay
- RNA Sequencing
- NK cell polyfunctionality evaluation by single-cell cytokine profiling and calculation of PSI
- Metabolic studies
- *In vivo* xenograft studies

● QUANTIFICATION AND STATISTICAL ANALYSIS

SUPPLEMENTAL INFORMATION

Supplemental Information can be found online at <https://doi.org/10.1016/j.stem.2020.05.008>.

ACKNOWLEDGMENTS

We thank Dr. Dean Lee (Nationwide Children's Hospital) for providing artificial antigen presenting cells (aAPCs). We thank Jon Chen, Sean Mackay, Tom Cain, Jens Eberlein, and Brianna Flynn from Isoplexis for carrying out the polyfunctionality studies. We appreciate helpful discussion and assistance from all Kaufman lab members. K.-J.M. was supported by grants from the Norwegian Cancer Society, the Norwegian Research Council, the South-Eastern Norway Regional Health Authority and the KG Jebsen Center for Cancer Immunotherapy and Radium Hospitalets Legater. These studies were supported by NIH grants R01CA203348 and U01CA217885 (to D.S.K.) and California Institute for Regenerative Medicine (CIRM) grant DISC2-09615 (to D.S.K.).

AUTHOR CONTRIBUTIONS

Design and implementation of studies, acquisition and analysis of data, and writing and revision of manuscript: H.Z.; acquisition and analysis of data and review of manuscript: R.H.B.; acquisition of data: D.B.; acquisition and analysis of data: E.H.A.; acquisition of data: Z.W.; acquisition and analysis of data: H.J.H.; acquisition of data: Z.M.; acquisition of data: C.W.; review and revision of the manuscript: K.-L.G.; design of studies and review and revision of manuscript: K.-J.M.; design of studies, analysis of data, and review and revision of manuscript: D.S.K.

DECLARATION OF INTERESTS

D.S.K. is a consultant for Fate Therapeutics, has equity, and receives income. The terms of this arrangement have been reviewed and approved by the University of California, San Diego in accordance with its conflict of interest policies. He also has patents filed or issued related to this work. K.-J.M. consults for and receives research support from Fate Therapeutics. K.-L.G. is co-founder and has an equity interest in Vivace Therapeutics, Inc., and Oncolmmune, Inc. H.Z. has a patent filed related to this work.

Received: February 20, 2020
Revised: March 22, 2020
Accepted: May 14, 2020
Published: June 11, 2020

REFERENCES

- Assmann, N., O'Brien, K.L., Donnelly, R.P., Dyck, L., Zaiatz-Bittencourt, V., Loftus, R.M., Heinrich, P., Oefner, P.J., Lynch, L., Gardiner, C.M., et al. (2017). Srebp-controlled glucose metabolism is essential for NK cell functional responses. *Nat. Immunol.* **18**, 1197–1206.
- Bremm, M., Pfeffermann, L.M., Cappel, C., Katzki, V., Erben, S., Betz, S., Quaiser, A., Merker, M., Bonig, H., Schmidt, M., et al. (2019). Improving Clinical Manufacturing of IL-15 Activated Cytokine-Induced Killer (CIK) Cells. *Front. Immunol.* **10**, 1218.
- Cichocki, F., Wu, C.Y., Zhang, B., Felices, M., Tesi, B., Tuininga, K., Dougherty, P., Taras, E., Hinderlie, P., Blazar, B.R., et al. (2018). ARID5B regulates metabolic programming in human adaptive NK cells. *J. Exp. Med.* **215**, 2379–2395.
- Cong, J., Wang, X., Zheng, X., Wang, D., Fu, B., Sun, R., Tian, Z., and Wei, H. (2018). Dysfunction of Natural Killer Cells by FBP1-Induced Inhibition of Glycolysis during Lung Cancer Progression. *Cell Metab.* **28**, 243–255.e5.
- Delconte, R.B., Kolesnik, T.B., Dagley, L.F., Rautela, J., Shi, W., Putz, E.M., Stannard, K., Zhang, J.G., Teh, C., Firth, M., et al. (2016). C1S is a potent checkpoint in NK cell-mediated tumor immunity. *Nat. Immunol.* **17**, 816–824.
- Denman, C.J., Senyukov, V.V., Somanchi, S.S., Phatarpekar, P.V., Kopp, L.M., Johnson, J.L., Singh, H., Hurton, L., Maiti, S.N., Huls, M.H., et al. (2012). Membrane-bound IL-21 promotes sustained ex vivo proliferation of human natural killer cells. *PLoS ONE* **7**, e30264.
- Dolstra, H., Roeven, M.W.H., Spanholtz, J., Hangalapura, B.N., Tordoir, M., Maas, F., Leenders, M., Bohme, F., Kok, N., Trilsbeek, C., et al. (2017). Successful Transfer of Umbilical Cord Blood CD34(+) Hematopoietic Stem and Progenitor-derived NK Cells in Older Acute Myeloid Leukemia Patients. *Clin. Cancer Res.* **23**, 4107–4118.
- Donnelly, R.P., Loftus, R.M., Keating, S.E., Liou, K.T., Biron, C.A., Gardiner, C.M., and Finlay, D.K. (2014). mTORC1-dependent metabolic reprogramming is a prerequisite for NK cell effector function. *J. Immunol.* **193**, 4477–4484.
- Felices, M., Lenvik, A.J., McElmurry, R., Chu, S., Hinderlie, P., Bendzick, L., Geller, M.A., Tolar, J., Blazar, B.R., and Miller, J.S. (2018). Continuous treatment with IL-15 exhausts human NK cells via a metabolic defect. *JCI Insight* **3**, e96219.
- Floros, T., and Tarhini, A.A. (2015). Anticancer Cytokines: Biology and Clinical Effects of Interferon- α 2, Interleukin (IL)-2, IL-15, IL-21, and IL-12. *Semin. Oncol.* **42**, 539–548.
- Fu, L., Liu, Y., An, Q., Zhang, J., Tong, Y., Zhou, F., Lu, W., Liang, X., and Gu, Y. (2019). Glycolysis metabolic changes in sperm cryopreservation based on a targeted metabolomic strategy. *Int. J. Clin. Exp. Pathol.* **12**, 1775–1781.
- Gardiner, C.M. (2019). NK cell metabolism. *J. Leukoc. Biol.* **105**, 1235–1242.
- Geller, M.A., Cooley, S., Judson, P.L., Ghebre, R., Carson, L.F., Argenta, P.A., Jonson, A.L., Panoskaltis-Mortari, A., Curtsinger, J., McKenna, D., et al. (2011). A phase II study of allogeneic natural killer cell therapy to treat patients with recurrent ovarian and breast cancer. *Cytotherapy* **13**, 98–107.
- Hilton, D.J., Richardson, R.T., Alexander, W.S., Viney, E.M., Willson, T.A., Sprigg, N.S., Starr, R., Nicholson, S.E., Metcalf, D., and Nicola, N.A. (1998). Twenty proteins containing a C-terminal SOCS box form five structural classes. *Proc. Natl. Acad. Sci. USA* **95**, 114–119.
- Hodgins, J.J., Khan, S.T., Park, M.M., Auer, R.C., and Ardolino, M. (2019). Killers 2.0: NK cell therapies at the forefront of cancer control. *J. Clin. Invest.* **129**, 3499–3510.
- Huntington, N.D., Legrand, N., Alves, N.L., Jaron, B., Weijer, K., Plet, A., Corcuff, E., Mortier, E., Jacques, Y., Spits, H., and Di Santo, J.P. (2009). IL-15 trans-presentation promotes human NK cell development and differentiation in vivo. *J. Exp. Med.* **206**, 25–34.
- Kawalekar, O.U., O'Connor, R.S., Fraietta, J.A., Guo, L., McGettigan, S.E., Posey, A.D., Jr., Patel, P.R., Guedan, S., Scholler, J., Keith, B., et al. (2016). Distinct Signaling of Coreceptors Regulates Specific Metabolism Pathways and Impacts Memory Development in CAR T Cells. *Immunity* **44**, 380–390.
- Keppel, M.P., Saucier, N., Mah, A.Y., Vogel, T.P., and Cooper, M.A. (2015). Activation-specific metabolic requirements for NK Cell IFN- γ production. *J. Immunol.* **194**, 1954–1962.
- Kershaw, N.J., Murphy, J.M., Liao, N.P.D., Varghese, L.N., Laktyushin, A., Whitlock, E.L., Lucet, I.S., Nicola, N.A., and Babon, J.J. (2013). SOCS3 binds specific receptor-JAK complexes to control cytokine signaling by direct kinase inhibition. *Nat. Struct. Mol. Biol.* **20**, 469–476.
- Khor, C.C., Vannberg, F.O., Chapman, S.J., Guo, H., Wong, S.H., Walley, A.J., Vukcevic, D., Rautanen, A., Mills, T.C., Chang, K.C., et al. (2010). CISH and susceptibility to infectious diseases. *N. Engl. J. Med.* **362**, 2092–2101.
- Knorr, D.A., Ni, Z., Hermanson, D., Hexum, M.K., Bendzick, L., Cooper, L.J., Lee, D.A., and Kaufman, D.S. (2013). Clinical-scale derivation of natural killer cells from human pluripotent stem cells for cancer therapy. *Stem Cells Transl. Med.* **2**, 274–283.
- Kobayashi, T., and Mattarollo, S.R. (2019). Natural killer cell metabolism. *Mol. Immunol.* **115**, 3–11.
- Li, Y., Hermanson, D.L., Moriarty, B.S., and Kaufman, D.S. (2018). Human iPSC-Derived Natural Killer Cells Engineered with Chimeric Antigen Receptors Enhance Anti-tumor Activity. *Cell Stem Cell* **23**, 181–192.e5.
- Mah, A.Y., and Cooper, M.A. (2016). Metabolic Regulation of Natural Killer Cell IFN- γ Production. *Crit. Rev. Immunol.* **36**, 131–147.
- Mao, Y., van Hoef, V., Zhang, X., Wennerberg, E., Lorent, J., Witt, K., Masvidal, L., Liang, S., Murray, S., Larsson, O., et al. (2016). IL-15 activates mTOR and primes stress-activated gene expression leading to prolonged antitumor capacity of NK cells. *Blood* **128**, 1475–1489.
- Marçais, A., Cherfils-Vicini, J., Viant, C., Degouve, S., Viel, S., Fenis, A., Rabilloud, J., Mayol, K., Tavares, A., Bienvenu, J., et al. (2014). The metabolic checkpoint kinase mTOR is essential for IL-15 signaling during the development and activation of NK cells. *Nat. Immunol.* **15**, 749–757.
- Marçais, A., Marotel, M., Degouve, S., Koenig, A., Fauteux-Daniel, S., Drouillard, A., Schlums, H., Viel, S., Besson, L., Allatif, O., et al. (2017). High mTOR activity is a hallmark of reactive natural killer cells and amplifies early signaling through activating receptors. *eLife* **6**, e26423.
- Michelet, X., Dyck, L., Hogan, A., Loftus, R.M., Duquette, D., Wei, K., Beyaz, S., Tavakkoli, A., Foley, C., Donnelly, R., et al. (2018). Metabolic reprogramming of natural killer cells in obesity limits antitumor responses. *Nat. Immunol.* **19**, 1330–1340.
- Miller, J.S., and Lanier, L.L. (2019). Natural Killer Cells in Cancer Immunotherapy. *Annu. Rev. Cancer Biol.* **3**, 77–103.
- Miller, J.S., Soignier, Y., Panoskaltis-Mortari, A., McNearney, S.A., Yun, G.H., Fautsch, S.K., McKenna, D., Le, C., Defor, T.E., Burns, L.J., et al. (2005). Successful adoptive transfer and in vivo expansion of human haploidentical NK cells in patients with cancer. *Blood* **105**, 3051–3057.
- Miller, J.S., Morishima, C., McNeel, D.G., Patel, M.R., Kohrt, H.E.K., Thompson, J.A., Sondel, P.M., Wakelee, H.A., Disis, M.L., Kaiser, J.C., et al. (2018). A First-in-Human Phase I Study of Subcutaneous Outpatient Recombinant Human IL15 (rhIL15) in Adults with Advanced Solid Tumors. *Clin. Cancer Res.* **24**, 1525–1535.
- Morvan, M.G., and Lanier, L.L. (2016). NK cells and cancer: you can teach innate cells new tricks. *Nat. Rev. Cancer* **16**, 7–19.
- O'Brien, K.L., and Finlay, D.K. (2019). Immunometabolism and natural killer cell responses. *Nat. Rev. Immunol.* **19**, 282–290.
- Palmer, D.C., Guittard, G.C., Franco, Z., Crompton, J.G., Eil, R.L., Patel, S.J., Ji, Y., Van Panhuys, N., Klebanoff, C.A., Sukumar, M., et al. (2015). Cish actively silences TCR signaling in CD8+ T cells to maintain tumor tolerance. *J. Exp. Med.* **212**, 2095–2113.
- Pearce, E.L., Poffenberger, M.C., Chang, C.H., and Jones, R.G. (2013). Fueling immunity: insights into metabolism and lymphocyte function. *Science* **342**, 1242454.
- Pomeroy, E.J., Hunzeker, J.T., Kluesner, M.T., Crosby, M.R., Lahr, W.S., Bendzick, L., Miller, J.S., Webber, B.R., Geller, M.A., Walcheck, B., et al.

- (2018). A Genetically Engineered Primary Human Natural Killer Cell Platform for Cancer Immunotherapy. *bioRxiv*. <https://doi.org/10.1101/430553>.
- Pomeroy, E.J., Hunzeker, J.T., Kluesner, M.G., Lahr, W.S., Smeester, B.A., Crosby, M.R., Lonetree, C.L., Yamamoto, K., Bendzick, L., Miller, J.S., et al. (2020). A Genetically Engineered Primary Human Natural Killer Cell Platform for Cancer Immunotherapy. *Mol. Ther.* 28, 52–63.
- Porter, D.L., Hwang, W.T., Frey, N.V., Lacey, S.F., Shaw, P.A., Loren, A.W., Bagg, A., Marcucci, K.T., Shen, A., Gonzalez, V., et al. (2015). Chimeric antigen receptor T cells persist and induce sustained remissions in relapsed refractory chronic lymphocytic leukemia. *Sci. Transl. Med.* 7, 303ra139.
- Poznanski, S.M., and Ashkar, A.A. (2019). What Defines NK Cell Functional Fate: Phenotype or Metabolism? *Front. Immunol.* 10, 1414.
- Putz, E.M., Guillerey, C., Kos, K., Stannard, K., Miles, K., Delconte, R.B., Takeda, K., Nicholson, S.E., Huntington, N.D., and Smyth, M.J. (2017). Targeting cytokine signaling checkpoint CIS activates NK cells to protect from tumor initiation and metastasis. *Oncot Immunology* 6, e1267892.
- Ran, F.A., Hsu, P.D., Lin, C.Y., Gootenberg, J.S., Konermann, S., Trevino, A.E., Scott, D.A., Inoue, A., Matoba, S., Zhang, Y., and Zhang, F. (2013). Double nicking by RNA-guided CRISPR Cas9 for enhanced genome editing specificity. *Cell* 154, 1380–1389.
- Ranson, T., Vosshenrich, C.A.J., Corcuff, E., Richard, O., Müller, W., and Di Santo, J.P. (2003). IL-15 is an essential mediator of peripheral NK-cell homeostasis. *Blood* 101, 4887–4893.
- Rautela, J., Surgenor, E., and Huntington, N.D. (2018). Efficient genome editing of human natural killer cells by CRISPR RNP. *bioRxiv*. <https://doi.org/10.1101/406934>.
- Romee, R., Rosario, M., Berrien-Elliott, M.M., Wagner, J.A., Jewell, B.A., Schappe, T., Leong, J.W., Abdel-Latif, S., Schneider, S.E., Willey, S., et al. (2016). Cytokine-induced memory-like natural killer cells exhibit enhanced responses against myeloid leukemia. *Sci. Transl. Med.* 8, 357ra123.
- Romee, R., Cooley, S., Berrien-Elliott, M.M., Westervelt, P., Verneris, M.R., Wagner, J.E., Weisdorf, D.J., Blazar, B.R., Ustun, C., DeFor, T.E., et al. (2018). First-in-human phase 1 clinical study of the IL-15 superagonist complex ALT-803 to treat relapse after transplantation. *Blood* 131, 2515–2527.
- Rossi, J., Paczkowski, P., Shen, Y.W., Morse, K., Flynn, B., Kaiser, A., Ng, C., Gallatin, K., Cain, T., Fan, R., et al. (2018). Preinfusion polyfunctional anti-CD19 chimeric antigen receptor T cells are associated with clinical outcomes in NHL. *Blood* 132, 804–814.
- Sun, L., Jin, Y.Q., Shen, C., Qi, H., Chu, P., Yin, Q.Q., Li, J.Q., Tian, J.L., Jiao, W.W., Xiao, J., and Shen, A.D. (2014). Genetic contribution of *CISH* promoter polymorphisms to susceptibility to tuberculosis in Chinese children. *PLoS ONE* 9, e92020.
- Wagner, J., Pfannenstiel, V., Waldmann, A., Bergs, J.W.J., Brill, B., Huenecke, S., Klingebiel, T., Rödel, F., Buchholz, C.J., Wels, W.S., et al. (2017). A Two-Phase Expansion Protocol Combining Interleukin (IL)-15 and IL-21 Improves Natural Killer Cell Proliferation and Cytotoxicity against Rhabdomyosarcoma. *Front. Immunol.* 8, 676.
- Wegiel, B., Vuerich, M., Daneshmandi, S., and Seth, P. (2018). Metabolic Switch in the Tumor Microenvironment Determines Immune Responses to Anti-cancer Therapy. *Front. Oncol.* 8, 284.
- Wrangle, J.M., Velcheti, V., Patel, M.R., Garrett-Mayer, E., Hill, E.G., Ravenel, J.G., Miller, J.S., Farhad, M., Anderton, K., Lindsey, K., et al. (2018). ALT-803, an IL-15 superagonist, in combination with nivolumab in patients with metastatic non-small cell lung cancer: a non-randomised, open-label, phase 1b trial. *Lancet Oncol.* 19, 694–704.
- Xue, Q., Bettini, E., Paczkowski, P., Ng, C., Kaiser, A., McConnell, T., Kodrasi, O., Quigley, M.F., Heath, J., Fan, R., et al. (2017). Single-cell multiplexed cytokine profiling of CD19 CAR-T cells reveals a diverse landscape of polyfunctional antigen-specific response. *J. Immunother. Cancer* 5, 85.
- Zhang, J.G., Farley, A., Nicholson, S.E., Willson, T.A., Zugaro, L.M., Simpson, R.J., Moritz, R.L., Cary, D., Richardson, R., Hausmann, G., et al. (2015). Correction for Zhang et al., The conserved SOCS box motif in suppressors of cytokine signaling binds to elongins B and C and may couple bound proteins to proteasomal degradation. *Proc. Natl. Acad. Sci. USA* 112, E2979.
- Zhu, H., and Kaufman, D.S. (2019). An Improved Method to Produce Clinical-Scale Natural Killer Cells from Human Pluripotent Stem Cells. *Methods Mol. Biol.* 2048, 107–119.
- Zhu, H., Lai, Y.S., Li, Y., Blum, R.H., and Kaufman, D.S. (2018). Concise Review: Human Pluripotent Stem Cells to Produce Cell-Based Cancer Immunotherapy. *Stem Cells* 36, 134–145.
- Zhu, H., Blum, R.H., Bjordahl, R., Gaidarova, S., Rogers, P., Lee, T.T., Abujarour, R., Bonello, G.B., Wu, J., Tsai, P.F., et al. (2020). Pluripotent stem cell-derived NK cells with high-affinity noncleavable CD16a mediate improved antitumor activity. *Blood* 135, 399–410.

STAR★METHODS

KEY RESOURCES TABLE

REAGENT or RESOURCE	SOURCE	IDENTIFIER
Antibodies		
APC-CD34	BD Biosciences	Cat#345804 RRID: AB_2686894
PE-CD45	BD Biosciences	Cat#555483 RRID: AB_395875
PE-CD43	BD Biosciences	Cat#560199 RRID:AB_1645655
PE-CD31	BD Biosciences	Cat# 340297 RRID:AB_400016
APC-CD56	BD Biosciences	Cat#555518 RRID: AB_398601
PE-CD56	BD Biosciences	Cat#5555516 RRID:AB_395906
FITC-CD94	BD Biosciences	Cat#555888 RRID:AB_396200
APC-CD117	eBiosciences	Cat#17117842. RRID:AB_2016658
PE-CD107a	BD Biosciences	Cat#555801 RRID:AB_396135
PE-NKG2D	BD Biosciences	Cat#561815 RRID: AB_10896282
PE-NKp46	BD Biosciences	Cat#557991 RRID: AB_396974
PE-NKp44	BD Biosciences	Cat#558563 RRID: AB_647239
PE-TRAIL	BD Biosciences	Cat#565499 RRID:AB_2732871
PE-FAS Ligand	BD Biosciences	Cat#564261 RRID:AB_2738713
PE-CD16	BD Biosciences	Cat#560995 RRID:AB_10562387
PacBlue-IFN-g	Biolegend	Cat#502522 RRID: AB_893525
APC-CD2	BD Biosciences	Cat#560642 RRID:AB_1727443
PE-CD57	BD Biosciences	Cat# 560844 RRID:AB_2033965
PE-NKG2C	R&D Systems	Cat# FAB138P RRID:AB_2132983
PE-NKG2A	Beckman Coulter	Cat# IM3291U RRID:AB_10643228
PE-CD158a,h	Beckman Coulter	Cat#A09778. RRID:AB_2801261
PE- CD158b1/b2,j	Beckman Coulter	Cat# IM2278U. RRID:AB_2728104
PE-CD158 e1/e2	Beckman Coulter	Cat# IM3292. RRID:AB_131339
PE-CD122	BD Biosciences	Cat#554522 RRID:AB_395451
PE-TRA-1-81	BD Biosciences	Cat#560161 RRID:AB_1645540
APC-SSEA4	Biolegend	Cat#330417 RRID:AB_2616818
Rabbit monoclonal anti-CIS (D4C10)	Cell Signaling Technology	Cat# 8431. RRID:AB_11179218
Mouse monoclonal anti-JAK1 (73/JAK1)	BD Biosciences	Cat# 610231. RRID:AB_397626
Rabbit monoclonal anti-phospho-JAK1 (Y1022 + Y1023) antibody [EPR1899(2)]	Abcam	Cat# ab138005. RRID:N/A
Rabbit monoclonal anti-STAT3 (D3Z2G)	Cell Signaling Technology	Cat# 12640. RRID:AB_2629499
Rabbit polyclonal anti-phospho-STAT3 (Tyr705)	Cell Signaling Technology	Cat# 9131. RRID:AB_331586
Mouse monoclonal anti-STAT5 (251619)	R&D System	Cat# MAB2174. RRID:AB_2239992
Rabbit monoclonal anti-phospho-STAT5 (Tyr694) (D47E7)	Cell Signaling Technology	Cat# 4322. RRID:AB_10544692
Rabbit monoclonal anti-phospho-p70 S6 Kinase (Thr389) (D5U1O)	Cell Signaling Technology	Cat# 97596. RRID:AB_2800283
Rabbit polyclonal anti-p70 S6 Kinase	Cell Signaling Technology	Cat# 9202. RRID:AB_331676
Rabbit monoclonal anti-phospho-S6 Ribosomal Protein (Ser235/236) (D57.2.2E)	Cell Signaling Technology	Cat# 4858. RRID:AB_916156
Rabbit monoclonal anti-S6 Ribosomal Protein (5G10)	Cell Signaling Technology	Cat# 2217. RRID:AB_331355
Rabbit monoclonal anti-GAPDH (D16H11)	Cell Signaling Technology	Cat# 5174. RRID:AB_10622025
Rabbit monoclonal anti- Vinculin (E1E9V)	Cell Signaling Technology	Cat# 13901. RRID:AB_2728768
Bacterial and Virus Strains		
pKT2-mCAG-IRES-GFPZEO	Branden Moriarity lab	N/A
pCMV(CAT)T7-SB100	Addgene	Cat#34879

(Continued on next page)

Continued

REAGENT or RESOURCE	SOURCE	IDENTIFIER
pSpCas9	GenScript	PX165
pGS-gRNA	GenScript	N/A
Biological Samples		
Human Serum AB	Sigma-Aldrich	Cat#H4522
Peripheral blood buffy coat	San Diego Blood Bank (https://www.sandiegobloodbank.org/)	N/A
Chemicals, Peptides, and Recombinant Proteins		
Recombinant human IL-2	Proleukin	Cat#NDC-66483-116-07
Recombinant human IL-3	Pepro Technology	Cat#200-03
Recombinant human IL-7	R&D Systems	R&D Systems Cat#207-IL
Recombinant human IL-15	R&D Systems	Cat#247-IL
Recombinant human FLT-3 Ligand	Pepro Technology	Cat#300-19
Recombinant human SCF	R&D Systems	Cat#255-SC/CF
Recombinant human VEGF	R&D Systems	Cat#293-VE
Recombinant human BMP-4	R&D Systems	Cat#314-BP
Recombinant human bFGF basic	R&D Systems	Cat#4114-TC
Recombinant human IL-12	R&D Systems	Cat#219-IL-005
Recombinant human IL-18	R&D Systems	Cat#9124-IL-010
a-MEM culture medium	Fisher Scientific	Cat#12634
Horse serum	Fisher Scientific	Cat#16050130
Fetal bovine serum	Fisher Scientific	Cat# 10437010
CellEvent Caspase-3/7 Green Detection Reagent	Thermo fisher	Cat#C10423
IncuCyte Caspase-3/7 Green Apoptosis Assay	Essenbioscience	Cat#4440
GolgiStop	BD Biosciences	Cat#554724
GolgiPlug	BD Biosciences	Cat#555029
Rapamycin	Sigma	Cat#R8781
STEMdiff APEL2 Medium	StemCell Technologies, Inc.	Cat#05270
CellTrace Violet Cell Proliferation Kit	Thermo fisher	Cat#C34571
CellTrace Far Red Cell Proliferation Kit	Thermo fisher	Cat#C34564
Critical Commercial Assays		
EasySep Human NK Cell Enrichment Kit	StemCell Technologies, Inc.	Cat#19055
Human Stem Cell Nucleofector™ Kit	Lonza	Cat# VPH-5012
Seahorse XF Glycolytic Rate Assay Kit	Agilent	Cat# 103344-100
Seahorse XF Cell Mito Stress Test Kit	Agilent	Cat# 103015-100
Deposited Data		
RNA sequencing	This paper	Accession number: GEO: GSE150155
Experimental Models: Cell Lines		
Human: iPS cells	Dan S. Kaufman lab	N/A
Human: K-562 cells	ATCC	Cat#CCL-243
Human: SKOV-3 cells	ATCC	Cat#HTB-77
Human: MOL-M13 cells	DSMZ	Cat#ACC 554
aAPC	Dean A. Lee lab	N/A
Experimental Models: Organisms/Strains		
Mouse: NOD.Cg-Prkdcscid Il2rgtm1Wjl/SzJ	Jackson lab	Cat#005557
Oligonucleotides		
gRNAs targeting exon 3 of human <i>CISH</i> gene: crRNA-1#: CAAGGGCTGCATGACTGGCT	This paper	N/A
gRNAs targeting exon 3 of human <i>CISH</i> gene: crRNA-2#: TGCTGGGGCCTTCTCGAGG	This paper	N/A

(Continued on next page)

Continued

REAGENT or RESOURCE	SOURCE	IDENTIFIER
Software and Algorithms		
IncuCyte real-time image system	Essenbioscience	N/A
Xenogen IVIS imaging system	Caliper Life Science	N/A
NovoExpress software	ACEA Biosciences	N/A
Cytobank	Cytobank	N/A
Seahorse Wave Desktop Software	Agilent	N/A
Prism 8	Graphpad	N/A

RESOURCE AVAILABILITY

Lead Contact

- Further information and requests for resources and reagents should be directed to and will be fulfilled by the Lead Contact, Dan S. Kaufman (dskaufman@ucsd.edu).

Materials Availability

- This study did not generate new unique plasmids/mouse lines/reagents.

Data and Code Availability

- The published article includes all datasets generated or analyzed during this study.
- RNA sequencing data is available in GEO via accession number: GEO: GSE150155.

EXPERIMENTAL MODEL AND SUBJECT DETAILS

Mouse Strain

8-10 weeks' female NOD/SCID/ γ C^{-/-} (NSG) mice (Jackson Laboratories, n = 5 per group) were used for *in vivo* experiments. After tumor cell inoculation, mice were randomly assigned to experimental groups. Mice were sacrificed when loss of ability to ambulate was observed. All mice were housed, treated, and handled in accordance with the guidelines set forth by the University of California, San Diego Institutional Animal Care and Use Committee and the National Institutes of Health's Guide for the Care and Use of Laboratory Animals.

Cells

hiPSC were generated from umbilical cord blood CD34⁺ cells (from female donor) and cultured as previously described (Knorr et al., 2013; Zhu and Kaufman, 2019). K562 (leukemia cell line established from a female patient with chronic myelogenous leukemia) and SKOV-3 (Ovarian cancer cell line derived from female patient with adenocarcinoma) were obtained from American Type Culture Collection (ATCC, Manassas, Virginia, U.S.). MOLM-13 (leukemia cell line derived from male patient with AML) cells were obtained from the DSMZ (Braunschweig, Germany). Primary human mononuclear cells were isolated through density gradient centrifugation from an apheresis product (San Diego Blood Center, from both female and male donors).

METHOD DETAILS

Cell culture

hiPSC were passaged using Accutase (STEMCELL Technologies, Vancouver, Canada, Cat. 07920) at a ratio of 1:4 to 1:10 on Matrigel (Corning, NY, U.S. Cat. 354277) coated plates, and cells were not allowed to reach full confluency prior to passaging (Knorr et al., 2013; Zhu and Kaufman, 2019). SKOV-3 were sub-cultured according to ATCC recommendations. K562 and MOLM-13 cells were maintained in RPMI 1640 (Thermo Fisher Scientific, Waltham, MA, 11875085) with 10% FBS. MOLM-13 cells were engineered to stably express luciferase and green fluorescent protein (GFP) using a pKT2-IRES-GFP:zeo plasmid in conjunction with a *SleepingBeauty* cassette (Addgene, Cambridge, Massachusetts) by nucleofection as previously described (Li et al., 2018).

Generation, identification and karyotyping of clonal CISH^{-/-} iPSC

Deletion of *CISH* in iPSCs was done using CRISPR/Cas9 technology. We designed a pair of gRNAs targeting exon 3 of *CISH* gene: crRNA-1#: CAAGGGCTGCATGACTGGCT, crRNA-2#: TGCTGGGGCCTTCCTCGAGG; DNA templates for gRNA were synthesized and cloned into pGS-gRNA (GenScript, Inc). pSpCas9 (GenScript PX165, 2 μ g), pGS-gRNA-1# (1 μ g) and gRNA-2# (1 μ g) were co-transfected to iPSC using Nucleofector™ 2b (Lonza, AAB-1001) with Human Stem Cell Nucleofector™ Kit (Lonza, VPH-5012).

24 hours after transfection, cells were selected with puromycin (2.5 $\mu\text{g}/\text{ml}$) (Sigma P8833) for 3 days. Then cells were seeded to 96-well plate at concentration of 1 cell/ml (100 μl per well) for single clone selection. Mutations in *CISH* gene were identified by Sanger sequencing using the following primer sets: 5'-CCAGCCAGAGGTCATGAAAC, 5'-ACCAGATTCCTCGAAGGTAGG. Identified *CISH* KO clones were verified as single-cell clone by amplifying the target region (same primer sets as sequencing) and TA cloning. Karyotype characterization was done using twenty G-banded metaphase cells by Cell Line Genetics Inc.

Derivation and expansion of NK cells from WT and *CISH*^{-/-} iPSCs

The derivation of NK cells from iPSCs has been previously described (Zhu and Kaufman, 2019). Briefly, 8,000 iPSCs were seeded in 96-well round-bottom plates with APEL media containing 40 ng/ml human Stem Cell Factor (SCF), 20 ng/ml human Vascular Endothelial Growth Factor (VEGF), 20 ng/ml recombinant human Bone Morphogenetic Protein 4 (BMP-4), and 10 μM rho kinase inhibitor (ROCK inhibitor, Y27632, Sigma). After 6 days of hematopoietic differentiation, spin embryoid bodies (EBs) were then directly transferred into each well of uncoated 6-well plates under NK cell differentiation conditions. NK cell differentiation conditions have previously been reported supplementing media with 5 ng/mL IL-3 (first week only), 10 ng/mL IL-15, 20 ng/mL IL-7, 20 ng/mL SCF, and 10 ng/mL flt3 ligand for 21-35 days. Half-media changes were performed weekly. NK cells were harvested after they reached maturity and co-cultured with irradiated K562-mb1L-21-4-1BB artificial antigen presenting cells (aAPCs) for expansion (Denman et al., 2012) with media containing RPMI 1640 and 10% FBS supplemented with 50 units/mL of hIL-2. aAPCs were kindly provided by Dr. Dean A. Lee (Nationwide Children's Hospital).

Isolation and expansion of PB-NK cells

Mononuclear cells were isolated through density gradient centrifugation from an apheresis product (San Diego Blood Center), and NK cells were enriched by depleting CD3⁺ and CD19⁺ cells using EasySep Human NK Cell Enrichment Kit (StemCell Technologies, Inc., 19055). Use of peripheral blood mononuclear cells from donors was approved by the Committee on the Use of Human Subjects in Research at the University of California, San Diego. PB-NK cells were expanded using the same method as used for expansion of iPSC-NK cells.

Immunoblotting

Immunoblotting was performed following standard methods from BioRad. Briefly, SDS-PAGE gels were used to resolve the cell lysates, and proteins were transferred to PVDF membranes using the wet transfer method. The detailed information of the antibodies is provided in Key Resources Table. All the antibody were used at 1:1000 dilution.

Flow cytometry

Flow cytometry was done on a NovoCyte (ACEA Biosciences) and data were analyzed using NovoExpress or FloJo software. The antibodies used for flow cytometry are listed in the Antibody section.

Mass cytometry

For viability assessment, cells were stained with Cell-ID Intercalator-103Rh (Fluidigm, San Francisco, CA, 201103B) in complete medium for 20 minutes at 37°C. Maxpar Cell Staining Buffer (Fluidigm, 201068) was used for all antibody staining and subsequent washing. Samples were incubated with Fc receptor binding inhibitor (Thermo Fisher Scientific, 14-9161-73) for 10 minutes at room temperature, before adding surface antibodies and incubating for 30 minutes at 4°C. Subsequently, cells were fixed in Maxpar PBS (Fluidigm, 201058) with 2% paraformaldehyde, transferred to methanol and stored at -20°C. The day after, cells were stained with an intracellular antibody cocktail for 40 minutes at 4°C and labeled with Cell-ID Intercalator-Ir (Fluidigm, 201192B). Samples were supplemented with EQ Four Element Calibration Beads (Fluidigm, 201078) and acquired on a CyTOF 2 (Fluidigm) equipped with a SuperSampler (Victorian Airship, Alamo, CA) at an event rate of < 500/sec. Antibodies were either obtained pre-labeled from Fluidigm or conjugated with metal isotopes using Maxpar X8 antibody labeling kits (Fluidigm) (Table S1). FCS files were normalized using Helios software (Fluidigm) and gated on CD45⁺ CD19⁻ CD14⁻ CD32⁻ CD3⁻ viable single cells using Cytobank (Cytobank Inc., Santa Clara, CA). For subsequent analysis, data was imported into R (R Core Team, 2019) using the *flowCore* package, and transformed using *arcsinh(x/5)*. 20,000 events were randomly sampled from each file and concatenated. t-Distributed Stochastic Neighbor Embedding (t-SNE) was then performed using the *Rtsne* R package with default settings and the following parameters: 2B4, CD16, CD161, CD2, CD27, CD3, CD34, CD38, CD56, CD57, CD8, CD94, DNAM-1, Granzyme B, LILRB1, Ki-67, KSP37, NKG2A, NKG2C, NKG2D, NKp30, Perforin, Siglec-7, Syk, TIGIT and TIM-3. Results were visualized using the *ggplot2* R package.

CD107a expression and IFN- γ staining:

NK cells were harvested, washed with their culture media and co-cultured with tumor targets at a 1:1 effector-to-target ratio. Different combinations of NK cells, tumors, stimulation molecules and antibodies were incubated with anti-CD107a PE (BD Biosciences, Franklin Lakes, NJ, 555801) for 1 hour. Following incubation, 1:1000 Golgi Stop and 1:1000 Golgi Plug solutions (BD Biosciences, 554724, 555029) were added and the cells incubated for an additional 2 hours. Cells were then counterstained with Live/Dead Fixable Aqua Dye (Thermo Fisher Scientific, L34957), IgG1 Isotype APC (BD Biosciences, 551442) and CD56-APC (BD Biosciences, 555518) for 30 min at 4°C. After staining, the cells were washed with buffer containing DPBS (Lonza, Basel, Switzerland, 17-512), 2% standard

FBS (Life Technologies, 10100147), 0.1% NaN₃ (Sigma Aldrich, 71289) and then fixed with BD Cytotfix (BD Biosciences, 554655) for 20 min at 4°C. Next, cells were washed and permeabilized using BD Perm/Wash (BD Biosciences, 554723) for 15 min at 4°C. Afterward, cells were stained for 30 min with IFN- γ Pacific Blue (Biolegend, San Diego, CA, 502521). After washing, cells were analyzed.

CellEvent Caspase-3/7 Green Flow Cytometry assay

Target cells were pre-stained with CellTrace Violet (Thermo-Fisher Scientific, C34557) at a final concentration of 5 μ M in PBS for 15 min at 37°C. After staining, the cells were washed in complete culture medium prior to being mixed with NK cell cultures at the indicated effector to target (E:T) ratios. After a brief centrifugation, co-cultures were incubated at 37°C for 3.5 hrs. Afterward, CellEvent® Caspase-3/7 Green Detection Reagent (Thermo Fisher Scientific, C10423) was added for an additional 30 min of culture for a total incubation time of 4 hours. During the final 5 minutes of staining, SYTOX AADvanced dead cell stain solution (Thermo Fisher Scientific, S10349) was added and mixed gently. Cells were then analyzed by flow cytometry.

IncuCyte Caspase-3/7 Green Apoptosis assay

Target cells were labeled with CellTrace™ Far Red (ThermoFisher, C34564). Adherent target cells were seeded in a 96-well plate at a density of 4000 cells/well 24 hr before addition of IncuCyte Caspase-3/7 Green Apoptosis Assay Reagent (Essen Bioscience, 4440) to each well diluted by a factor of 1,000. Non-adherent target cells were seeded in fibronectin coated 96-well plates at a density of 30,000 to 50,000 cells/well and further incubated at room temperature for 30 min before the addition of IncuCyte Caspase-3/7 Green Apoptosis Assay Reagent. After incubation, NK cells were added at various E:T ratios and monitored on the IncuCyte ZOOM to acquire images every 1 h for adherent cells and every 30 min for non-adherent cells. Experiments were performed with 3 independent biological triplicates. The cytotoxicity of target cells was analyzed by quantifying red cell number and/or overlay of Caspase 3/7 (green) within the red cells.

RNA Sequencing

Total RNA was isolated from cells using the miRNeasy Kit (QIAGEN) according to the manufacturer's protocol. RNA quality control, library construction, sequencing and data analysis were performed by Novogene Inc. Briefly, RNA quantification and qualification was performed using Nanodrop for checking RNA purity (OD260/OD280), agarose gel electrophoresis and Agilent 2100 for checking RNA integrity. mRNA was purified from total RNA using poly-T oligo-attached magnetic beads. cDNA library was synthesized using random hexamer primer and M-MuLV Reverse Transcriptase and sequencing using Illumina HiSeq 2000. The threshold of differential expression genes in Volcano diagram is $\text{padj} < 0.05$. Color descending from red to blue in heatmap of differential expression genes indicated $\log_{10}(\text{FPKM}+1)$ from large to small. ClusterProfiler software was used for all enrichment analysis, including Gene Ontology (GO) enrichment, Disease Ontology (DO) enrichment and Kyoto Encyclopedia of Genes and Genomes (KEGG, <https://www.kegg.jp/>). $\text{padj} < 0.05$ was considered as significant enrichment.

NK cell polyfunctionality evaluation by single-cell cytokine profiling and calculation of PSI

Single-cell cytokine profiling was analyzed using IsoPlexis 32-plex immune cytokine response panel as previously reported (Rossi et al., 2018; Xue et al., 2017). Briefly, cryopreserved NK cells were thawed and resuspended in complete media (RPMI+10%FBS) with 5 ng/ml IL-15 at a density of 1×10^6 cells/ml. Cells were recovered at 37°C, 5% CO₂ overnight. Next day, cells were stimulated with IL-12 (10 ng/ml, R&D System, 219-IL-005) and IL-18 (100 ng/ml, R&D System, 9124-IL-010) for 1 hour then cells were loaded into the single-cell barcode chip (SCBC) microchip for single-cell secretomics evaluation. A single cell functional profile was determined for each NK cell type. Profiles were categorized into effector (Granzyme B, IFN- γ , MIP-1 α , Perforin, TNF- α , TNF- β), stimulatory (GM-CSF, IL-2, IL-5, IL-7, IL-8, IL-9, IL-12, IL-15, IL-21), regulatory (IL-4, IL-10, IL-13, IL-22, TGF- β 1, sCD137, sCD40L), chemoattractive (CCL-11, IP-10, MIP-1 β , RANTES), and inflammatory (IL-1b, IL-6, IL-17A, IL-17F, MCP-1, MCP-4) groups. Polyfunctional NK cells were defined as cells co-secreting at least 2 proteins from the prespecified panel per cell coupled with the amount of each protein produced (ie, combination of number of proteins secreted and at what intensity). Polyfunctional strength index (PSI) was defined as the percentage of polyfunctional cells, multiplied by mean fluorescence intensity (MFI) of the proteins secreted by those cells, calculated using a prespecified formula (Rossi et al., 2018).

Metabolic studies

WT iPSC-NK cells and *CISH*^{-/-} iPSC NK cells were incubated with low concentration of IL-15 (1 ng/ml) for 7 days with or without rapamycin (100 ng/ml) (Sigma, R8781). Cells were resuspended in Seahorse XF Assay Medium (Agilent Technologies) and seeded at 150,000 cells/well (96-well plate). Plate was pre-coated with Poly-D-Lysine (Sigma, P6407) over-night at 37°C. The extracellular acidification rate and the oxygen consumption rate were measured (pmoles/min) in real time in an XFe96 analyzer using Seahorse XF Glycolytic Rate Assay Kit (Agilent, 103344-100) and Seahorse XF Cell Mito Stress Test Kit (Agilent, 103015-100). Basal glycolysis was measured before the addition of rotenone/antimycin A (0.5 μ M) and glycolytic was elucidated by subtracting the rate of glycolysis before and after addition of 2-deoxy-D-glucose (2DG, 100 mM). Basal respiration was measured after addition of glucose, ATP-linked respiration was calculated from subtraction of basal respiration and respiration after addition of oligomycin (1 μ M), and mitochondrial spare respiratory capacity (SRC) was measured after addition of carbonyl cyanide-4 (trifluoromethoxy)phenylhydrazine (FCCP, 1 μ M).

***In vivo* xenograft studies**

Mice were sub-lethally irradiated (225 cGy) 1 day prior to tumor engraftment. Mice were given 1×10^6 luc-expressing MOLM-13 cells via Intravenous (IV). NK cells (10^7 cells/mouse) were injected IV 1 day after tumor cells infusion. NK cells were supported by the injection of IL-2 and/or IL-15 as reported previously (Li et al., 2018). Tumor burden was determined by BLI using the Xenogen IVIS Imaging system. 7 days or 14 days after infusion of NK cells, 50 μ l blood was collected from mice tail vein and red blood cells were removed by ACK lysing buffer (GIBCO, A10492). The remaining cells were subjected to flow cytometric staining of human CD56-APC (BD Biosciences, 555518) or CD45-PE (BD Biosciences, 555483). Human NK cell persistence in PB was calculated as number of human CD56⁺ or CD45⁺ cells per μ l blood.

QUANTIFICATION AND STATISTICAL ANALYSIS

Data are presented as the mean \pm standard error of the mean. Differences between groups were evaluated using the one-way ANOVA or Two-tailed t test (noted in figure legends). For the quantification of *in vivo* image, data are presented as the mean \pm SEM and differences between groups were analyzed using Two-tailed t test. Survival curve was analyzed using Log-rank (Mantel-Cox) test. Statistical analysis is performed in the environment of GraphPad Prism Statistical. All tests were considered significant at $p < 0.05$.